Multichannel topological Kondo models and their low-temperature conductances

Guangjie Li,[1,2] Elio J. König,[3,4] and Jukka I. Väyrynen[1]

[1]*Department of Physics and Astronomy, Purdue University, West Lafayette, Indiana 47907, USA.*
[2]*Department of Physics and Astronomy, University of Utah, Salt Lake City, Utah 84112, USA.*
[3]*Department of Physics, University of Wisconsin-Madison, Madison, Wisconsin 53706, USA*
[4]*Max-Planck Institute for Solid State Research, 70569 Stuttgart, Germany*

(Dated: August 6, 2025)

In the multichannel Kondo effect, overscreening of a magnetic impurity by conduction electrons leads to a frustrated exotic ground state. It has been proposed that multichannel topological Kondo (MCTK) model involving topological Cooper pair boxes with M Majorana modes [SO(M) "spin"] and N spinless electron channels exhibits an exotic intermediate coupling fixed point. This intermediate fixed point has been analyzed through large-N perturbative calculations, which gives a zero-temperature conductance decaying as $1/N^2$ in the large-N limit. However, the conductance at this intermediate fixed point has not been calculated for generic N. Using representation theory, we verify the existence of this intermediate-coupling fixed point and find the strong-coupling effective Hamiltonian for the case $M = 4$. Using conformal field theory techniques for SO(M), we generalize the notion of overscreening and conclude that the MCTK model is an overscreened Kondo model. We find the fixed-point finite-size energy spectrum and the leading irrelevant operator (LIO). We express the fixed-point conductance in terms of the modular S-matrix of SO(M) for general N, confirming the previous large-N result. We describe the finite-temperature corrections to the conductance by the LIO and find that they are qualitatively different for the cases $N = 1$ and $N \geq 2$ due to the different fusion outcomes with the current operator. We also compare the multichannel topological Kondo model to the topological symplectic Kondo model.

CONTENTS

I. INTRODUCTION

The Kondo model explains the local minimum resistivity at low temperatures in certain noble metals using a spin-spin exchange interaction between the magnetic impurity and conduction electrons [1]. The multichannel generalization of it [2] with fruitful experimental developments in mesoscopic devices [3–9] leads Kondo physics to a new era due to not only the experimental measurement of conductance, but also the potential applications to topological quantum computations using emergent anyonic excitations [10–15]. The key requirement is overscreening: the impurity spin (S) is smaller than the largest possible local total spin ($N/2$) for N-channel conduction electrons. Overscreening indicates an intermediate coupling fixed point [2], whose existence was verified in the large-N limit where the intermediate coupling fixed point

moves toward weak coupling and becomes perturbatively accessible in the $1/N$ expansion [16].

The intermediate coupling fixed point of the $N \geq 2$-channel Kondo model is an exotic state not described by free electrons. As first demonstrated using the Bethe Ansatz technique [17, 18] the impurity entropy is $S_\text{imp} = \ln[g(N)]$ where the generally irrational number $g(N) = 2\cos[\pi/(N+2)]$ can be interpreted as the effective ground state degeneracy of the impurity problem. Crucially, it coincides with the quantum dimension of the anyon "1/2", labeled by its representation in the $\text{SU}(2)_N$ fusion category [10]. As shown by Emery and Kivelson [19] (see also Refs. [20–22]) for the two-channel Kondo (2CK) model, an emergent Majorana at the impurity spin will be decoupled from the conduction electrons.

Since the 1990s (multichannel) Kondo physics has also been realized in artificial quantum emulators. Of particular relevance are strongly interacting quantum dots coupled to electronic leads [4]. In this context, while there has been progress towards measuring the entropy of a mesoscopic device [23–25], a somewhat more natural experimental observable than the impurity entropy is the (trans-)conductance across the dot. Crucially, at zero temperature it takes an N-dependent universal value, while the conductance correction near $T = 0$ is given by the leading perturbation, namely the least irrelevant operator (LIO). The first-order correction $T^{\Delta_\text{LIO}-1}$ with $\Delta_\text{LIO} = 1 + 2/(N+2)$ dominates unless it vanishes in which case one considers the second-order correction $T^{2(\Delta_\text{LIO}-1)}$ [5, 7]. In any case, the temperature dependence demonstrates non-Fermi liquid behavior, i.e., non-T^2 behavior. Here, the LIO is formed by the first descendants of the adjoint (spin-1) primary operators [10, 26–33].

Theoretically, further platforms of Kondo effects in mesoscopic devices with non-Fermi liquid behavior have been proposed for setups with symmetry groups [34] other than SU(2). These include $\text{SO}(M)$, e.g. the (multichannel) topological Kondo model whose impurity consists of M Majorana zero modes on a floating topological superconducting island coupled to normal spin-polarized metallic leads [35–39], as well as $\text{Sp}(2k)$, e.g. the topological symplectic Kondo model whose impurity consists of k one-dimensional topological end states that are coupled to spinful leads [40–42]. The existence of the intermediate coupling fixed point of the topological symplectic Kondo model has been demonstrated through the strong coupling analysis [40]. However the strong coupling of the $\text{SO}(M)$ topological Kondo model has not been well studied and thus the existence of the intermediate coupling fixed point has not been fully demonstrated generally for any M, although the mapping from the $M = 3, 4$ topological Kondo models to the MCK models and the large-N results of the N-channel topological Kondo model both indicate its existence [35, 37]. In this paper we show that the strong-coupling fixed point of the $\text{SO}(M)$ topological Kondo model is indeed unstable, suggesting flow towards an intermediate fixed point. We will also clarify the meaning of overscreening in the topological Kondo model.

Another open question that we will address in this work concerns the low-temperature conductance. The low-temperature conductance correction calculated in the large-N

limit is $T^{(M-2)/(2N)}$ [37], which suggests T^Δ where $\Delta = (M-2)/(2N+M-2)$ is the scaling dimension for the adjoint primary operator. The first descendant of this primary operator gives the LIO with scaling dimension $1 + \Delta$. However, it is also known that the $N = 1$ topological Kondo model has a conductance correction $T^{2\Delta}$ [35, 36, 43], which seems contradictory to the above. A similar change in the temperature exponent of the conductance correction occurs in the multichannel charge-Kondo effect [8, 44]. In this paper, by developing the boundary conformal field theory for the topological Kondo model, we address the reason for this change in the temperature exponent.

This manuscript is structured as follows. In Sec. II, we first analyze the $\text{SO}(M)$ topological Kondo exchange interaction using representation theory and show that it is an overscreened Kondo interaction which supports the existence of the intermediate coupling fixed point. In Sec. III, we introduce the conformal field theory techniques and the Kac-Moody algebra for the topological Kondo intermediate coupling fixed point. In Sec. IV, by identifying the important operators from the intermediate fixed point, we give the analytical results of the zero temperature conductance and the finite-temperature conductance correction for the N-channel topological Kondo model with M Majoranas. In Sec. V, we further discuss the analogous conductance correction of the topological $\text{Sp}(2k)$ Kondo model.

II. INSTABILITY OF THE STRONG COUPLING FIXED POINT FOR SO(M) KONDO MODELS

The total Hamiltonian $H_0 + H_\text{MCTK}$ of the N channel topological Kondo model consists of the linearized kinetic energy of the itinerant fermions (H_0), and the N-channel $\text{SO}(M)$ topological Kondo interaction H_MCTK (see Fig. 1a):

$$H_0 = \frac{v_\text{F}}{2\pi} \int_{-l}^{l} \mathrm{d}x \sum_{n=1}^{N} \sum_{\alpha=1}^{M} \mathrm{i}\, \psi_{n,\alpha}^\dagger(x)\partial_x \psi_{n,\alpha}(x), \quad (1)$$

$$H_\text{MCTK} = \lambda \sum_{n=1}^{N} \sum_{A} S^A J_n^A(x=0), \quad (2)$$

where v_F is the Fermi velocity and $2l$ is the length of the system, which can be taken to infinity at the end [45]. Here, we considered the right mover as a continuation of the left mover to the negative axis [10, 45] (see Fig. 1b-c). The $\text{SO}(M)$ impurity operators are $S^{A=(\alpha,\beta)} = -\mathrm{i}\gamma_\alpha\gamma_\beta/2$ with $\gamma_{1,...,M}$ denoting the M Majorana zero modes. The conduction electron operators in the nth channel are $J_n^{A=(\alpha,\beta)} = -\mathrm{i}(\psi_{n,\alpha}^\dagger\psi_{n,\beta} - \psi_{n,\beta}^\dagger\psi_{n,\alpha})$ and there are $M(M-1)/2$ (α,β) pairs that satisfy $\alpha < \beta$ when $\alpha,\beta = 1,\ldots,M$ label flavors. The operators S^A and J_n^A are different representations of the $\text{SO}(M)$ generators.

A weak Kondo coupling $\lambda > 0$ flows to the stronger coupling under renormalization group (RG) flow [35] (see Fig. 1d). For simplicity we consider an idealized case of only one Kondo coupling, i.e. fully isotropic exchange; while weak flavor anisotropies are irrelevant under the RG flow [35, 37,
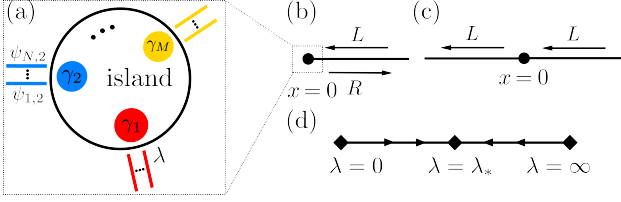
FIG. 1. (a) Setup of the multichannel topological Kondo model implemented as a Coulomb blockaded Majorana island with M Majoranas (flavors) coupled to N metallic leads (channels) for each Majorana. (b) Each channel is assumed to host linearly dispersing left (L) and right (R) moving modes on a half axis, coupled to the impurity at $x = 0$. (c) Unfolding to chiral model: The right movers can be considered as a continuation of the left movers defined on the full axis, see Eq. (1). (d) The RG flow of the Kondo coupling λ.

46], channel anisotropy is not [37]. In the large-N limit, in Ref. [37] some of us perturbatively calculated the RG equations and found that there is a stable intermediate coupling fixed point $\lambda_* = 1/(2N\rho)$ where $\rho = 1/(\pi v_F)$ is the constant density of states per length. This intermediate-coupling fixed point indicates an unstable strong-coupling fixed point (see Fig. 1d). However, the perturbative results can no longer be trusted in the case $N \sim \mathcal{O}(1)$, where the intermediate fixed point (if any) no longer resides in the weak coupling regime.

Here we first evince the presence of the intermediate nontrivial fixed point. Trivially, as for any Kondo problem, the fixed point $\lambda = 0$ is unstable (because λ is marginally relevant). Next we consider $\lambda = \infty$ and study if this fixed point is stable or not. To this end, we assume dominant H_{MCTK}, Eq. (2), in the strong coupling regime and momentarily neglect kinetic energy, Eq. (1) [2]. In the lattice version of Fig. 1b, x takes discrete values $0, 1, 2, \ldots$ and 0 denotes the closest site to the impurity. At $x = 0$, we notice that

$$J^A = -\mathrm{i}(\gamma_{\alpha,R}\gamma_{\beta,R} + \gamma_{\alpha,I}\gamma_{\beta,I})/2 \equiv S_R^A + S_I^A, \quad (3)$$

when introducing Majorana representation $\psi_\alpha = (\gamma_{\alpha,R} + \mathrm{i}\gamma_{\alpha,I})/2$ for each conduction electron channel n (the channel index n is omitted). Thus, the impurity represented by operator S^A is screened by conduction electrons represented by $2N$ S^As (see also [47–49] for the case of single conduction S^A). Since two S^As can combine into a singlet, see Eq. (9), this means that Eq. (2) is an overscreened Kondo interaction. This overscreening in terms of the number of S^A indicates the instability of the strong-coupling fixed point and therefore leads to a stable intermediate-coupling fixed point. By analogy with the 2CK model, i.e., when the Majorana island is screened by two conduction Majorana channels, we expect that the ground states of Eq. (2) with $N = 1$ form a new impurity that is represented by S^A and will be further screened by the next nearest ($x = 1$) conduction electrons.

The above analogy can be shown by solving the ground states of Eq. (2) using the following standard Casimir form:

$$\sum_A S^A J^A = \frac{1}{2}\left[\sum_A (S^A + J^A)^2 - (S^A)^2 - (J^A)^2\right]. \quad (4)$$

These three operators on the right are the Casimir operators, and the Casimir invariant $c(R)$ for each Casimir operator is determined by its representation R. In terms of the Dynkin's labels a_i (non-negative integers), i.e., $R = \sum_{i=1}^r a_i\mu_i$ where the integer r is the rank of the Lie algebra [$r = m$ for SO($M = 2m$) and SO($M = 2m + 1$)] and μ_i are the fundamental representations, the Casimir invariant is

$$c(R) = \sum_{i,j=1}^m (\alpha_i \cdot \alpha_i)(a_i/2 + 1)(C^{-1})_{ij}a_j. \quad (5)$$

The vector α_i are the simple roots and the matrix $C_{ij} \equiv 2(\alpha_i \cdot \alpha_j)/(\alpha_i \cdot \alpha_i)$ is the Cartan matrix [50–53]. Thus, the ground states and their energy of Eq. (4) are both determined by the representations of S^A and J^A.

Before going to the representation theory, one can calculate the Casimir invariant of S^A using only the commutation relations $\{\gamma_i, \gamma_j\} = 2\delta_{ij}$:

$$\sum_A (S^A)^2 = -\sum_{\alpha<\beta} \gamma_\alpha\gamma_\beta\gamma_\alpha\gamma_\beta/4 = M(M-1)/8. \quad (6)$$

This result can be verified by plugging the Dynkin's labels of $R(S^A)$ (see Appendix A),

$$R(S^A) = \begin{cases} \mu_{m-1} \oplus \mu_m, & \text{if } M = 2m \\ \mu_m, & \text{if } M = 2m + 1 \end{cases} \quad (7)$$

into Eq. (5), which also results in the right side of Eq. (6). For the following part in this section, we focus on the even case $M = 2m$. The representations μ_{m-1} and μ_m are the two spinor fundamental representations which have the same dimension 2^{m-1} but different total parities $\Pi_{\alpha=1}^{2m}\gamma_\alpha = \pm 1$.

In order to obtain the Casimir invariant for J^A, we note that $J^A(x = 0)$ commutes with the number operator and thus is block diagonal in the single-site $x = 0$ Fock space. Therefore $R(J^A)$ is a reducible representation. Consequently, we introduce the K-particle sector at the site $x = 0$ and define $J^{A,K}$ the corresponding block in J^A. The dimension of the K-particle representation $R(J^{A,K})$ is $\binom{2m}{K}$. The total dimension of $R(J^A)$ is $\sum_{K=0}^{2m}\binom{2m}{K} = 2^{2m}$ where $0 \leq K \leq M$; this total dimension agrees with what we expect from Eq. (3).

The K-particle sector and $M - K$-particle sector are identical due to particle-hole symmetry. This can be seen from the Casimir operator for J^A in the K-particle sector

$$\sum_A J^{A,K}J^{A,K} = \sum_{\alpha\neq\beta} \psi_\alpha^\dagger\psi_\alpha(1-\psi_\beta^\dagger\psi_\beta) = K(M-K). \quad (8)$$

The second equality above is obtained by noting that for any K-particle state, in order to have a nonzero average for $\psi_\alpha^\dagger\psi_\alpha(1-\psi_\beta^\dagger\psi_\beta)$, α should be one of the K occupied flavors, and β should be one of the $M - K$ unoccupied flavors. In total, there are $K(M - K)$ (α,β) pairs. Eq. (3) means that the representation $R(J^A)$ can be given by $R(S_R^A) \otimes R(S_I^A)$ and thus we get the representations of J^A for SO($M = 2m$) (see Appendix A):

$$R(J^A) = R(S^A) \otimes R(S^A) \equiv \bigoplus_{K=0}^{2m} R(J^{A,K}) \quad (9)$$

using the representation $R(S^A)$, i.e., Eq. (7). We check that Eq. (8) matches the result by plugging the Dynkin's labels of $R(J^{A,K})$ [Eq. (9)] into Eq. (5).

Now, we can decompose $R(S^A) \otimes R(J^{A,K})$ for each K-particle sector. While the corresponding Casimir invariant can be evaluated, its full expression is too complex to show here, but the reader can refer to Appendix A 2 for more information. Nevertheless, we find that μ_{m-1} and μ_m have the smallest Casimir invariant $c(R)$ [Eq. (6)] except the trivial representation $R = 0$ and always exist in the decompositions of $R(S^A) \otimes R(J^{A,K})$ for any $0 \leq K \leq 2m$. Thus, the ground states of Eq. (2) lie in the $K = m$-particle sector (half-filling), where Eq. (8) is maximal and Eq. (4) has its minimum. These ground states labeled by $\mu_{m-1} \oplus \mu_m$ form a new impurity [same representation as the original impurity, see Eq. (7)]. We thus expect by symmetry that it couples to conduction electrons as in Eq. (2) and thus will be screened by the electrons at site $x = 1$, which confirms that the leads can be considered as two-channel Majorana-lead according to Eq. (3), which will overscreen the Majorana-island just as in the conventional 2CK effect. Moreover, the effective Hamiltonian of strong coupling is still a topological Kondo interaction but with a new Kondo coupling $\lambda' \sim t^2/\lambda$ where t is the kinetic energy of the itinerant electrons. The strong coupling limit of λ is the weak coupling limit of λ', which we know to be unstable. This weak-strong duality predicts a self-dual point, which is the intermediate fixed point (see Fig. 1d). We show an explicit example in the Appendix B for $M = 4$ and $N = 1$. The ground states in the strong coupling fixed point are in the $K = m = 2$-particle sector, which can be represented by two decoupled spin-1s (a six-dimensional space formed by placing $K = 2$ particles into $M = 4$ available orbitals). The impurity can be represented by two decoupled spin-1/2s. Thus, the 1-channel topological SO(4) Kondo model is equivalent to 2CK and is overscreened. This equivalence comes from the fact SO(4) $\sim$ SU(2) $\times$ SU(2) (see Appendix B 1 and the supplementary material of Ref. [37]). Similar arguments about overscreening from the strong-coupling perspective are also used in Refs. [2, 54, 55].

The multichannel case ($N > 1$) with more screening is also an overscreened Kondo model. In conclusion, we have shown the instability of the strong-coupling fixed point and thus the existence of the intermediate-coupling fixed point (see the $\lambda = \lambda_*$ point in Fig. 1d).

III. CONFORMAL FIELD THEORY AT THE INTERMEDIATE-COUPLING FIXED POINT

The powerful boundary conformal field theory method was successfully applied to the intermediate-coupling fixed point of the multichannel SU(2) Kondo model [10, 27–29, 31, 45]. As we verified the strong-coupling instability of the multichannel SO(M) topological Kondo model in the last section, suggesting the existence of an intermediate-coupling fixed point, we introduce in this section the SO(M) generalization of the conformal field theory description.

A. The definition of overscreening

Below Eq. (3) we argued that the topological Kondo model is overscreened. In this section we make this notion more precise. Recall that overscreening in the N-channel (spin-1/2 conduction electrons) SU(2) Kondo model with impurity spin-s means $2s < N$ [2]. This constraint for the impurity spin is also the cut-off for the allowed spins (representations) in the SU(2)$_N$ affine Lie algebra, i.e., the Kac-Moody algebra, which is part of the conformal field theory describing the intermediate-coupling fixed point [10]. Thus, we can think of overscreening as the requirement that the impurity representation is allowed in the affine Lie algebra. We note however the following two exceptions: (i) the case $s = N/2$ corresponding to exact or perfect screening, and (ii) the (trivial) case of a scalar impurity [spin-0], which are both allowed in the Kac-Moody algebra but flow to the same free fermion theory as the free fixed point. Next, we generalize the definition of overscreening using the representation cut-off for the SO(M) case.

The symmetry current operator for the N-channel SO(M) Kondo model, Eq. (2), is defined as

$$\widetilde{J}^A(x) = \sum_{n=1}^N J_n^A = \sum_{n=1}^N \sum_{\alpha,\beta=1}^M \psi_{n,\alpha}^\dagger(x)(T^A)_{\alpha\beta}\psi_{n,\beta}(x),$$
(10)

where T^As are the traceless generators of the SO(M) group, defined as $(T^A)_{\alpha\beta} \equiv (T^{rs})_{\alpha\beta} = i(\delta_\alpha^r \delta_\beta^s - \delta_\beta^r \delta_\alpha^s)$. Here the generators are labeled by the pair r, s of indices $r < s = 1, ..., M$. We may alternatively label the generators by a single integer $A = 1, ..., M(M-1)/2$. The generators satisfy $\text{Tr}(T^A T^B) = 2\delta^{AB}$ and $[T^A, T^B] = i\sum_C f^{ABC}T^C$ where $f^{ABC} = (-i/2)\text{Tr}([T^A, T^B]T^C)$ is the structure constant. The Kac-Moody algebra for the Fourier components of Eq. (10) is

$$[\widetilde{J}_p^A, \widetilde{J}_{p'}^B] = i\sum_C f^{ABC}\widetilde{J}_{p+p'}^C + 2N p\delta^{AB}\delta_{p,-p'},$$
(11)

with the prefactor in the second term defining the level $2N$ (see Appendix C). Thus, the affine Lie algebra for the N-channel topological Kondo model is SO(M)$_{2N}$ (see Ref. [56] for the $N = 1$ case) because each screening fermion channel is two screening Majorana channels as shown by Eq. (3). For N Majorana channels one finds SO(M)$_N$ [47].

By requiring primary states to have non-negative norm, we can find that the allowed representations $R = \sum_{i=1}^m a_i \mu_i = \vec{\ell}$ for the SO(M)$_{2N}$ Kac-Moody algebra must satisfy (see Appendix D 2 and D 3 for derivations)

$$\begin{cases} \ell_i \pm \ell_j \leq 2N, & \text{if } M = 2m \\ \ell_i \pm \ell_j \leq 2N \text{ and } \ell_j \leq 2N, & \text{if } M = 2m+1 \end{cases}$$
(12)

where $1 \leq i < j = 1, ..., m$, $a_i = \ell_i - \ell_{i+1}$, $i = 1, ..., m-1$ and

$$a_m = \begin{cases} \ell_{m-1} + \ell_m, & \text{if } M = 2m \\ 2\ell_m, & \text{if } M = 2m+1 \end{cases}.$$
(13)

0	μ_1	μ_2	$\mu_1 + \mu_2$	$2\mu_1$	$2\mu_2$	$2\mu_1 + \mu_2$	$\mu_1 + 2\mu_2$	$2\mu_1 + 2\mu_2$
1	$\sqrt{2}$	$\sqrt{2}$	2	1	1	$\sqrt{2}$	$\sqrt{2}$	1

TABLE I. The quantum dimensions for all the allowed representations in SO(4)$_2$, see Sec. III B. The anyons denoted by $\mu_{1,2}$ appear at the topological Kondo intermediate fixed point. The presence of quantum dimensions larger than one indicate overscreening. The trivial screening cases are given by the representations with quantum dimension 1.

The necessary requirements are thus that the Dynkin labels

$$a_{i=1,\ldots,m-1} \leq 2N, \text{ and, } a_m \leq \begin{cases} 2N, & \text{if } M = 2m \\ 4N, & \text{if } M = 2m+1 \end{cases}. \tag{14}$$

When the impurity representation satisfies all inequalities in Eq. (12) but upon fusion with the conduction electrons (see Sec. III B) still gives the free-fermion spectrum [45], we define this case as "trivial screening". The overscreening is when the representation satisfies Eq. (12) but does not belong to trivial screening. For the SU(2)$_N$ case, the trivial screening occurs when the impurity spin $s = 0$ or $N/2$. All other cases with spin $s = 1/2, 1, \ldots, (N-1)/2$ are overscreening. We can easily check that the impurity representation $R(S^A)$, i.e., Eq. (7) satisfy Eq. (12) for any $N \geq 1$ and does not belong to the trivial screening. Thus, we conclude that the multichannel topological Kondo model is an overscreened Kondo model which matches our conclusion in the last section that the strong-coupling fixed point is unstable.

B. Fusion rules, quantum dimensions, and scaling dimensions

The fusion rule for two allowed representations R_1 and R_2 of the Kac-Moody algebra is $R_1 \times R_2 = \sum_{R_3} N_{R_1 R_2}^{R_3} R_3$ where $N_{R_1 R_2}^{R_3} = \sum_{R_4} S_{R_1,R_4} S_{R_2,R_4} S_{R_3,R_4}^* / S_{0,R_4}$ by the Verlinde formula [57], S_{R_1,R_4} is the modular S-matrix for SO(M)$_{2N}$ [58] and $*$ denotes complex conjugation. (These SO(M)$_{2N}$ fusion rules for all pairs of representations define a fusion category [59].) Based on the fusion rule (see Appendix D for example), one can calculate the effective dimension for each representation, that is, the quantum dimension which is generally noninteger because of the cut-off Eq. (12). The quantum dimension is given by the modular S-matrix $g[R] = S_{0,R}/S_{0,0}$, and it further gives the impurity entropy [10, 60]

$$S_{\text{imp}} = \ln g[R(S^A)] = \ln g[\mu_m], \tag{15}$$

for the SO(M = 2m)$_{2N}$ and SO(M = 2m + 1)$_{2N}$ topological Kondo models, which matches with the $N = 1$ result in Ref. [61]. For example, the quantum dimensions for all the allowed representations of SO(4)$_2$ by Eq. (12) are listed in Tab. I. Because the representation of the impurity is μ_1 or μ_2 as shown by Eq. (7), the impurity entropy is $\ln \sqrt{2}$ for the SO(4)$_2$ topological Kondo model.

In order to obtain the scaling dimensions of leading operators in the Kondo intermediate fixed point, we now proceed

with the construction of the conformal field theory description. The kinetic energy H_0 [Eq. (1)] in its Sugawara form after non-Abelian bosonization [Eq. (10)] becomes [45, 60, 62]:

$$H_0 = \frac{\pi v_F}{l} \sum_{p=-\infty}^{\infty} \left[\sum_A \frac{: \widetilde{J}_{-p}^A \widetilde{J}_p^A :}{M + 2N - 2} + \sum_a \frac{: \widetilde{J}_{-p}^a \widetilde{J}_p^a :}{2N + M - 2} \right], \tag{16}$$

where $\widetilde{J}_p^A$ [$\widetilde{J}_p^a$] are the pth component from the Fourier transformation of the SO(M)$_{2N}$ [SO(2N)$_M$] generators; the normal ordering $: \cdots :$ moves operators with $p > 0$ to the right. The Kondo interaction H_{MCTK} [Eq. (2)] becomes

$$H_{\text{MCTK}} = \tilde{\lambda} \frac{\pi v_F}{l} \sum_{p=-\infty}^{\infty} \sum_A \widetilde{J}_p^A S^A, \tag{17}$$

where $\tilde{\lambda} = \rho\lambda = \lambda/(\pi v_F)$. At a critical value (the intermediate-coupling fixed point) $\tilde{\lambda} = \tilde{\lambda}_* = 2/(M + 2N - 2)$, the Kondo interaction H_{MCTK} can be absorbed into Eq. (16) by defining the currents $\mathcal{J}_p^A = \widetilde{J}_p^A + S^A$ which still satisfy the SO(M)$_{2N}$ Kac-Moody algebra Eq. (11) [10, 45]. However, this will only work if the representation obtained by fusing the impurity and conduction electron representations is in the Kac-Moody algebra, i.e., satisfies Eq. (12).

The most fundamental states in the spectrum of Eq. (16) are called primary states which are annihilated by $\widetilde{J}_{p>0}^A$ and $\widetilde{J}_{p>0}^a$. Excited states can be obtained from them by acting with $\widetilde{J}_{p<0}^A$ and $\widetilde{J}_{p<0}^a$ [45, 63]. Thus, the primary states can be labeled by the representations of the SO(M)$_{2N}$ and SO(2N)$_M$ Lie algebra. Another way to see this is from Eq. (16) which is in the standard Casimir form, so that its eigenvalues can be labeled by the representations of the SO(M)$_{2N}$ and SO(2N)$_M$ Lie algebra. For example, when $M = 4$ and $N = 1$, the primary states (see Tab. II) are labeled by the representations (Dynkin's label) of the SO(4) (a_1, a_2) and SO(2) (Q) Lie algebra. In the free fixed point, only vector representations (even $a_1 + a_2$) are allowed because the current operators Eq. (10) are defined using fermions and not Majoranas. The primary-state energies are [for $(M = 4, N = 1)$]

$$E_0^{(a_1,a_2,Q)} = \frac{\pi v_F}{l} \left[\frac{1}{8} \left(a_1 + \frac{a_1^2}{2} + a_2 + \frac{a_2^2}{2} \right) + \frac{1}{8} Q^2 \right]. \tag{18}$$

If we take $a_1 = 2j$ and $a_2 = 2j_f$, Eq. (18) becomes identical to the SU(2)$_2$ conformal data [45, 63]. The conformal scaling dimension of the primary operator that creates the primary state (a_1, a_2, Q) when applied to the vacuum is $E_0^{(a_1,a_2,Q)} l/(\pi v_F)$ (see Tab. II) [64].

By the Affleck-Ludwig *fusion hypothesis* [29, 30], the Kondo fixed point (the intermediate-coupling fixed point, see Fig. 1d) primary states are determined by fusion of the free fixed point primary states [45] with the representation of the impurity. For the case SO(4)$_2$, where the impurity representation is $R(S^A) = \mu_1 \oplus \mu_2$, see Tab. II. The allowed boundary operators are found from the free fixed point primary operators after double fusion with the impurity [45]. We are

a_1	a_2	$Q \bmod 4$	$E_0^{(a_1,a_2,Q)} l/\pi v_F$	multiplicity
0	0	0	0	1
1	1	1	$1/2$	1
2	0	2	1	1
0	2	2	1	1
2	2	0	1	1
1	1	3	$3/2$	1
a_1	a_2	$Q \bmod 4$	$E_0^{(a_1,a_2,Q)} l/\pi v_F$	multiplicity
1	0	0	$3/16$	1
0	1	1	$5/16$	1
2	1	1	$13/16$	1
1	0	2	$11/16$	1
1	2	2	$19/16$	1
1	2	0	$11/16$	1
0	1	3	$21/16$	1
2	1	3	$29/16$	1

TABLE II. Primary states/operators (a_1, a_2, Q) and their scaling dimensions $E_0^{(a_1,a_2,Q)} l/\pi v_F$ of the $SO(4)_2$ Kac-Moody algebra. Upper table: free fixed point. Lower table: Kondo fixed point obtained from free fixed point after single fusion with the impurity representation μ_1. The single fusion results with impurity μ_2 can be found by interchanging $a_1 \leftrightarrow a_2$.

particularly interested in the leading irrelevant boundary operator (LIO) that characterizes for instance finite-temperature corrections to observables near the Kondo intermediate fixed point. Although $R(S^A)$ is reducible, we only consider the fusions relevant to fixed fermion parity sectors, $\mu_1 \otimes \mu_1 \otimes (a_1\mu_1 + a_2\mu_2)$ and $\mu_2 \otimes \mu_2 \otimes (a_1\mu_1 + a_2\mu_2)$ (see the Appendix D 7 for the cross terms). The leading irrelevant operators are obtained from $a_1 = a_2 = 0$ and $a_1 = a_2 = 2$ with $Q = 0$. When $a_1 = a_2 = 0$ (the $a_1 = a_2 = 2$ case gives identical results), we get

$$\mu_{1,2} \otimes \mu_{1,2} \otimes 0 = 2\mu_{1,2} \oplus 0, \tag{19}$$

where $2\mu_1$ $(a_1 = 2, a_2 = 0, Q = 0)$ and $2\mu_2$ $(a_1 = 0, a_2 = 2, Q = 0)$ both have scaling dimension $1/2$, calculated from Eq. (18). These resulting primaries $2\mu_{1,2}$ transform under the adjoint representation of the $SO(4)$ Lie algebra.

In the next section, we discuss the conductance correction given by the LIO, which is the first descendant of adjoint primary fields $\vec{\phi}$, i.e., $\vec{J}_{-1} \cdot \vec{\phi}$ [29, 34]. In the $SO(4)_2$ case, these operators are $\vec{J}_{-1}^{2\mu_1} \cdot \vec{\phi}^{2\mu_1}$ and $\vec{J}_{-1}^{2\mu_2} \cdot \vec{\phi}^{2\mu_2}$ where $\vec{\phi}^{2\mu_{1,2}}$ are the dimension $1/2$ primary operators that correspond to the representations $2\mu_{1,2}$ in Eq. (19). The current operators $\vec{J}_{-1}^{2\mu_{1,2}}$ are the generators that transform under the representation $2\mu_{1,2}$ and their scaling dimensions are 1. Thus, the scaling dimension of the LIO $\vec{J}_{-1} \cdot \vec{\phi}$ for the case $SO(4)_2$ is $1 + 1/2 = 3/2$. Generally for any M, N, the scaling dimension for the LIO of the $SO(M)_{2N}$ case is [60]

$$\Delta_1 = 1 + \Delta_0 = 1 + \frac{M-2}{2N+M-2} \tag{20}$$

where $\Delta_n = n + \Delta_0$ is the scaling dimension of the corresponding nth descendant of the primary operator with scaling

dimension Δ_0. Special cases of Eq. (20) can be found in the $SO(3)_2$ Kondo model [35] which was mapped to the $SU(2)_4$ Kondo model, in the $SO(M)_2$ model [61, 65, 66], in the N-channel $SO(4)_{2N}$ model which was mapped to the $SU(2)_{2N}$ Kondo model [37], and in the perturbative large-N limit of the multichannel topological Kondo model [37].

IV. LOW-TEMPERATURE CONDUCTANCE

The low-temperature conductance near the intermediate-coupling fixed point can be calculated using conformal field theory techniques [4, 10, 35, 49, 67, 68]. The charge transport is determined by the conduction electron current in the leads; for flavor α and channel j, the current operator is $I_{j,\alpha} = I_{R;j,\alpha} - I_{L;j,\alpha}$ where the chiral currents are $I_{L,R;j,\alpha}(x) = ev_F\psi_{L,R;j,\alpha}^\dagger(x)\psi_{L,R;j,\alpha}(x)$ (see Fig. 1). One can calculate the linear response conductance by using the Kubo formula that involves the equilibrium current-current correlation functions, see Ref. [40] for details on a fully analogous calculation. For simplicity and practical relevance [37] we focus on charge transport in one of the channels, say $j = 1$. Because of charge conservation, it is sufficient to evaluate the off-diagonal elements of the conductance matrix $G_{\alpha\beta} = \lim_{V_\beta \to 0}\langle I_{1,\alpha}\rangle/V_\beta$ which characterizes the current in lead α generated by a weak voltage V_β in lead β. The presence of a Kondo impurity modifies only the correlation functions $\langle I_{L;1,\alpha} I_{R;1,\beta}\rangle$ between opposite chirality currents [67, 68]. We suppress the position and time arguments in the correlation functions for brevity [69]; this omission is not important for our derivations below.

A. Zero-temperature conductance

The channel and flavor symmetries exhibited by the Hamiltonian Eqs. (1)-(2) in both the free and Kondo fixed points restrict the current-current correlation functions to only two independent ones: $\langle I_{L;j,\alpha} I_{R;k,\alpha}\rangle = \delta_{jk}\langle I_{L;1,1} I_{R;1,1}\rangle$ and $\langle I_{L;j,\alpha} I_{R;k,\beta}\rangle = \delta_{jk}\langle I_{L;1,1} I_{R;1,2}\rangle$ for $\alpha \neq \beta$. At the Kondo fixed point, we can relate these two correlation functions to a single correlator evaluated at the free fixed point. In order to do this, we first define chiral $(\chi = L, R)$ densities that transform properly under $SO(M)$ rotations: $J_\chi^{(c)}(x) = \sum_j \vec{\psi}_{\chi;j}^\dagger(x) \cdot \vec{\psi}_{\chi;j}(x) = \sum_{j,\alpha} I_{L,R;j,\alpha}(x)$ which transforms as the representation 0 (singlet) and $J_\chi^{(d)}(x) = \sum_j \vec{\psi}_{\chi;j}^\dagger(x) D_1 \vec{\psi}_{\chi;j}(x) = \sum_j [I_{\chi;j,1}(x) - I_{\chi;j,2}(x)]$ which transforms as the representation $4\mu_1$ (or spin-2, see the supplementary materials of Ref. [35]) for $SO(3)$, $2\mu_1 + 2\mu_2$ for $SO(4)$, and $2\mu_1$ for $SO(M \geq 5)$. Here, $\vec{\psi}_{\chi;j} = (\psi_{\chi;j,1}, \ldots, \psi_{\chi;j,M})^T$ and $D_1 = \mathrm{diag}(1, -1, 0, \ldots, 0)$ (a symmetric traceless $M \times M$ matrix). Note that the density $J^{(d)}$ is one of the $M - 1 + M(M-1)/2$ densities given by the symmetric traceless $M \times M$ matrices (see Appendix E).

The current-current correlation functions can be written in

terms of the above density-density correlations functions:

$$\langle I_{L;1,1} I_{R;1,1} \rangle = \frac{1}{M^2 N} \langle J_L^{(c)} J_R^{(c)} \rangle + \frac{M-1}{2MN} \langle J_L^{(d)} J_R^{(d)} \rangle, \tag{21}$$

$$\langle I_{L;1,1} I_{R;1,2} \rangle = \frac{1}{M^2 N} \langle J_L^{(c)} J_R^{(c)} \rangle - \frac{1}{2MN} \langle J_L^{(d)} J_R^{(d)} \rangle. \tag{22}$$

These equations are true with or without Kondo interaction. At the free fixed point (denoted from hereon by subscript f), we have no flavor mixing so $\langle I_{L;1,1} I_{R;1,2} \rangle_{\mathrm{f}} = 0$ (leading to $G_{12} = 0$) and

$$\langle J_L^{(c)} J_R^{(c)} \rangle_{\mathrm{f}} = NM \langle I_{L;1,1} I_{R;1,1} \rangle_{\mathrm{f}}, \tag{23}$$

$$\langle J_L^{(d)} J_R^{(d)} \rangle_{\mathrm{f}} = 2N \langle I_{L,R;1,1} I_{L,R;1,1} \rangle_{\mathrm{f}}. \tag{24}$$

At the Kondo intermediate-coupling fixed point (denoted by subscript K), the density-density correlation function $\langle J_L^{(c,d)} J_R^{(c,d)} \rangle_{\mathrm{K}}$ is given by its free fixed point value multiplied by a constant factor that is fully determined by representation theory [10]. The density $J^{(c)}$ is a singlet and thus its factor will be 1; its correlation function is not modified by Kondo interaction. The density $J^{(d)}$ transforms non-trivially with a representation $R(J^{(d)})$ that depends on M [see above Eq. (21)]. The corresponding factor is given by the following modular S-matrix values [10, 64]:

$$\mathcal{S}_N(M) = \frac{S_{R(J^{(d)}),R(S^A)}/S_{R(J^{(d)}),0}}{S_{R(S^A),0}/S_{0,0}}. \tag{25}$$

In other words, $\langle J_L^{(c)} J_R^{(c)} \rangle_{\mathrm{K}} = \langle J_L^{(c)} J_R^{(c)} \rangle_{\mathrm{f}}$ and $\langle J_L^{(d)} J_R^{(d)} \rangle_{\mathrm{K}} = \mathcal{S}_N \langle J_L^{(d)} J_R^{(d)} \rangle_{\mathrm{f}}$. By using these relation in Eqs. (21)-(24), we get

$$\langle I_{L;1,1} I_{R;1,1} \rangle_{\mathrm{K}} = \frac{1 + (M-1)\mathcal{S}_N}{M} \langle I_{L;1,1} I_{R;1,1} \rangle_{\mathrm{f}}, \tag{26}$$

$$\langle I_{L;1,1} I_{R;1,2} \rangle_{\mathrm{K}} = \frac{1 - \mathcal{S}_N}{M} \langle I_{L;1,1} I_{R;1,1} \rangle_{\mathrm{f}}. \tag{27}$$

which relate the Kondo fixed point correlation functions to a single free fixed point correlation function. A similar relation holds for the zero-temperature conductance matrix elements [40]. Thus, the transconductance G_{12} of the N-channel SO(M) topological Kondo model is

$$\frac{G_{12}(N, M)}{G_0} = \frac{1 - \mathcal{S}_N(M)}{M}, \quad G_0 = e^2/h. \tag{28}$$

Unfortunately there is no simple closed formula for $\mathcal{S}_N(M)$ with general N and M [58]. We can nevertheless evaluate $\mathcal{S}_N(M)$ and G_{12} for any given N, M, see Fig. 2 for some small values. For $M = 3, 4, 5, 6, 7$ and generic N, we have

$$\mathcal{S}_N(3) = 1 - 2\cos\left(\frac{\pi}{2N+1}\right) + 2\cos\left(\frac{2\pi}{2N+1}\right), \tag{29}$$

$$\mathcal{S}_N(4) = 2\cos\left(\frac{\pi}{N+1}\right) - 1, \tag{30}$$

$$\mathcal{S}_N(5) = 2\cos\left(\frac{2\pi}{2N+3}\right) + \left[1 - 2\cos\left(\frac{\pi}{2N+3}\right)\right]^{-1}, \tag{31}$$

$$\mathcal{S}_N(6) = \cos\left(\frac{2\pi}{N+2}\right) \bigg/ \cos\left(\frac{\pi}{N+2}\right), \tag{32}$$

$$\mathcal{S}_N(7) = 2\cos\left(\frac{2\pi}{2N+5}\right)$$
$$+ \left[2\cos\left(\frac{\pi}{2N+5}\right) - 2\cos\left(\frac{2\pi}{2N+5}\right) - 1\right]^{-1}. \tag{33}$$

We will mention some special cases of Eq. (28) that have been previously discussed in the literature. In the conventional $N = 1$ topological Kondo model, one has $\mathcal{S}_{N=1} = -1$ and $G_{12} = (2/M)(e^2/h)$ for all M, which matches with previous results [35, 36, 43, 56, 66, 70, 71]. The result for $M = 3, 4$ and generic N can also be verified by mapping to previous results on the SU(2) multichannel Kondo effect. The N-channel SO(3) topological Kondo model can be mapped to the $4N$CK, i.e., SU(2)$_{4N}$ Kac-Moody algebra and the N-channel SO(4) topological Kondo model can be mapped to the $2N$CK, i.e., SU(2)$_{2N}$ Kac-Moody algebra at the intermediate coupling fixed point. After the mapping, we use the modular S-matrix for SU(2)$_k$ [10, 58, 72]

$$S_{j,s} = \sqrt{\frac{2}{k+2}} \sin\left[\frac{\pi(2j+1)(2s+1)}{k+2}\right]. \tag{34}$$

The representation of J^d is spin-2 ($j = 2$) for the SU(2)$_{4N}$ case and spin-1 ($j = 1$) for the SU(2)$_{2N}$ case. The representation of impurity is spin-1/2 ($s = 1/2$) for both cases. The $\mathcal{S}_N$s calculated from Eq. (34) match with Eqs. (29)-(30) that are calculated using the modular S-matrix of SO($M = 3, 4)_{2N}$.

Finally, we can comment on the limits $N, M \rightarrow \infty$ of Eq. (28). The perturbative large-N limit [37] can be seen from Eqs. (29)-(33) which yield $\lim_{N\rightarrow\infty} G_{12}(N, M = 3, \ldots, 7)/G_0 = \pi^2/(4N^2)$ (see Fig. 2b), matching with the large-N conductance of Ref. [37]. For a fixed N, we numerically show that the conductance vanishes as $2/(MN)$ in the large-M limit (see Fig. 2a). However, in perturbation theory in the Kondo interaction, the conductance G_{12} is proportional to $\tilde{\lambda}_*^2$ [37], which is $\tilde{\lambda}_*^2 \sim 1/M^2$ because $\tilde{\lambda}_* = 2/(M + 2N - 2) \sim 1/M$ in the large-M limit [see below Eq. (17)]. This mismatch of the large-M conductance between the conformal field theory method and the perturbation theory indicates that, unlike the large-N limit, the large-M limit is not perturbatively accessible.

B. Leading finite-temperature correction to the conductance

Next, we discuss the finite-temperature correction to the conductance, Eq. (28). This correction arises from the deviation $\tilde{\lambda} - \tilde{\lambda}_*$ of the Kondo coupling from its fixed point value, also known as correction to scaling [45]. We will show that the conductance correction depends on the channel number N
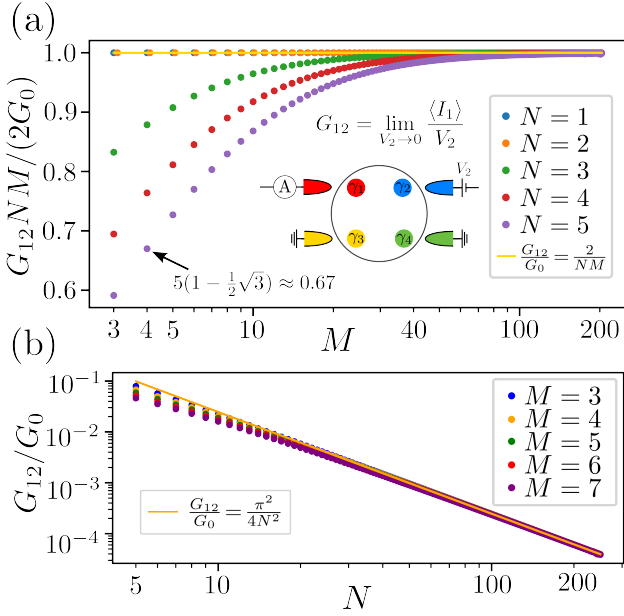
FIG. 2. (a) The zero-temperature conductance for $N = 1, \ldots, 5$ and $M = 3, \ldots, 203$. All the points above are given by analytical results Eq. (28) and Eq. (25) [for illustration the $(N, M) = (5, 4)$ point is shown explicitly]. The $N = 1, 2$ points are degenerate but we horizontally shifted the $N = 2$ points in order to show both of them. The inset shows the definition of an off-diagonal conductance matrix element for the case $N = 1, M = 4$. In the large-M limit, the conductance G_{12}/G_0 is asymptotically $2/(MN)$. (b) In the large-N limit, the conductance is asymptotically $\pi^2/(4N^2)$.

as,

$$
G_{12}(T) - G_{12}(0) \sim \begin{cases} T^{2(\Delta_1 - 1)}, & N = 1 \\ T^{(\Delta_1 - 1)}, & N \geq 2 \end{cases}, \quad (35)
$$

where Δ_1 is given by Eq. (20). The result Eq. (35) agrees with the cases $N = 1$ and $N \to \infty$ that were previously studied in the literature [35–37, 43, 56, 66, 70, 71].

The piecewise result Eq. (35) is due to different fusion results of the operator J^d for $N = 1$ and $N \geq 2$ cases, i.e.,

$$
R(J^{(d)}) \times R(J^{(d)}) = \begin{cases} 0, & N = 1 \\ 0 + \ldots, & N \geq 2 \end{cases}. \quad (36)
$$

The operator J^d is used to calculate the fixed point conductance by using Eqs. (21)-(22) and the conductance correction is given by the correction to $\langle J^d J^d \rangle$ due to the LIO $\vec{J}_{-1} \cdot \vec{\phi}$ with scaling dimension shown in Eq. (20). The first-order conductance correction is

$$
\lim_{\omega \to 0} \frac{-1}{\omega L} \int_{-\beta/2}^{\beta/2} d\tau \int_0^L dx' \int_{-\beta/2}^{\beta/2} d\tau_1 \, \mathrm{e}^{\mathrm{i}\omega\tau}
$$
$$
\langle \mathcal{T}_\tau J^{(d)}(x, \tau) J^{(d)}(x', 0) \vec{J}_{-1} \cdot \vec{\phi}(0, \tau_1) \rangle, \quad (37)
$$

where $\beta = 1/T$ and $\tau = \mathrm{i}t$ [40, 44, 73]. By power counting, each integral contributes T^{-1} and the correlation function contributes $\sim T^{2+\Delta_1}$. Thus, the first-order correction

Eq. (37) gives conductance correction $\sim T^{(\Delta_1 - 1)}$. This is the case in the multichannel $N \geq 2$ topological Kondo model [37] which allows fusion results other than 0. However, the first-order correction vanishes at $N = 1$ because the fusion rule, Eq. (36), of two J^ds gives only 0, i.e., $J^d J^d \sim \mathbb{I}$ and thus $\langle J^d J^d \vec{J}_{-1} \cdot \vec{\phi} \rangle \sim \langle \vec{J}_{-1} \cdot \vec{\phi} \rangle = 0$ (see also the supplementary materials of Ref. [35]). It means that the temperature dependence of the conductance correction for the 1-channel topological Kondo model arises from the second order in the LIO,

$$
\lim_{\omega \to 0} \frac{-1}{\omega L} \int_{-\beta/2}^{\beta/2} d\tau \int_0^L dx' \int_{-\beta/2}^{\beta/2} d\tau_1 \int_{-\beta/2}^{\beta/2} d\tau_2 \, \mathrm{e}^{\mathrm{i}\omega\tau}
$$
$$
\langle \mathcal{T}_\tau J^{(d)}(x, \tau) J^{(d)}(x', 0) \vec{J}_{-1} \cdot \vec{\phi}(0, \tau_1) \vec{J}_{-1} \cdot \vec{\phi}(0, \tau_2) \rangle, \quad (38)
$$

and is of order $T^{2(\Delta_1 - 1)} = T^{2(M-2)/M}$ [43, 56, 66].

V. COMPARISON TO THE SYMPLECTIC CASE

In the above sections, we mainly discussed the application of conformal field theory to calculate the conductance of the multichannel $\mathrm{SO}(M)$ topological Kondo model. One may wonder how these techniques are applicable to other Lie groups such as the recently studied symplectic $\mathrm{Sp}(2k)$ Kondo model [40, 41]. In the symplectic Kondo case, the low-temperature conductance correction was found to be the Fermi liquid T^2 [40, 41]. However, as we show below, this is only true for the $\mathrm{Sp}(4)_1$ case.

Due to a similar representation cutoff as Eq. (12), the allowed representations of the $\mathrm{Sp}(2k)_1$ Kac-Moody algebra are the fundamental ones $\mu_{i=1,\ldots,k}$ where μ_1 represents the impurity. The double fusion rule of the impurity μ_1 gives

$$
\mu_1 \otimes \mu_1 \otimes 0 = 2\!\!\!\diagdown\!\!\mu_1 \oplus \mu_2 \oplus 0 \quad (39)
$$

where $2\!\!\!\diagdown\!\!\mu_1$ means this adjoint representation $2\mu_1$ is not allowed by the Kac-Moody algebra (see also the supplemental material of Ref. [40]). Thus, the LIO $\vec{J}_{-1} \cdot \vec{\phi}^{2\mu_1}$ is not allowed in the boundary operators. However, one can consider high-order descendants and contract them with the representations allowed by the $\mathrm{Sp}(2k)_1$ Kac-Moody algebra. It turns out that the LIO is $(\overrightarrow{J_{-1} J_{-1}})^{\mu_2} \cdot \vec{\phi}^{\mu_2}$ with scaling dimension $\Delta_2^{\mu_2} = 2 + \Delta_0^{\mu_2}$ where $\Delta_0^{\mu_2} = k/(k+2)$. The operators $(\overrightarrow{J_{-1} J_{-1}})^{\mu_2}$ are the μ_2 operators constructed from the product of two $2\mu_1$ (the adjoint representation) operators J_{-1}. This construction always exits because of the following representation decomposition [53]:

$$
2\mu_1 \otimes 2\mu_1 = 4\mu_1 \oplus (2\mu_1 + \mu_2) \oplus 2\mu_1 \oplus 2\mu_2 \oplus \mu_2 \oplus 0. \quad (40)
$$

The μ_2 at the right site of Eq. (40) denotes the representation of $\overrightarrow{J_{-1} J_{-1}}$.

Similar to the $\mathrm{SO}(M)$ Kondo model, the charge conductance in the symplectic $\mathrm{Sp}(2k)$ case is determined by the operator J^d [see Eq. (21) for the $\mathrm{SO}(M)$ case], which transforms as the representation μ_2 of $\mathrm{Sp}(2k)$ [40]. The first-order low-temperature conductance correction resulting from the LIO

$(\overrightarrow{J_{-1}J_{-1}})^{\mu_2} \cdot \vec{\phi}^{\mu_2}$ is proportional to $T^{(\Delta_2^{\mu_2}-1)}$. As mentioned in Sec. IV, if the fusion rule of the operator J^d gives only a trivial representation 0, the first-order correction vanishes and one should consider the second-order perturbation. The fusion rule of the $\mathrm{Sp}(2k)_1$ affine Lie algebra is identical to that of the $\mathrm{SU}(2)_k$ affine Lie algebra: the impurity representation μ_1 of $\mathrm{Sp}(2k)_1$ is equivalent to the "1/2" of $\mathrm{SU}(2)_k$ and the μ_2 is equivalent to the "1" of $\mathrm{SU}(2)_k$ [see also Eq. (39) as a verification]. At $k=2$, we have $\mu_2 \otimes \mu_2 = 0$, which is equivalent to $1 \times 1 = 0$ in $\mathrm{SU}(2)_2$. Thus, one considers the second-order perturbation which would lead to $T^{2(\Delta_2^{\mu_2}-1)} = T^3$. However, this is subleading compared to the Fermi liquid correction T^2 given by the operator $\vec{J}^{2\mu_1} \cdot \vec{J}^{2\mu_1}$ [34]. When $k \geq 3$, one considers the first-order correction. Thus, the conductance correction of the $\mathrm{Sp}(2k)_1$ Kondo model is

$$\delta G(T) \sim \begin{cases} T^2, & k=2 \\ T^{(\Delta_2^{\mu_2}-1)} = T^{2\frac{k+1}{k+2}}, & k \geq 3 \end{cases}. \qquad (41)$$

Note that in the $\mathrm{Sp}(4)_1$ setup of Ref. [48, 49], the first-order conductance correction does not vanish because their conductance is not calculated using J^d and thus they obtain a non-Fermi liquid behavior $T^{(\Delta_2^{\mu_2}-1)} = T^{3/2}$ at $k = 2$. This difference in conductance correction between their $\mathrm{SO}(5)_1$ or $\mathrm{Sp}(4)_1$ Kondo model [48, 49] and the recently studied symplectic $\mathrm{Sp}(4)_1$ Kondo model [40, 41] is similar to the difference between the spin-2CK model and charge-2CK model [44].

Furthermore, in the multichannel $\mathrm{Sp}(2k)_{N \geq 2}$ case, the adjoint primary operator $\vec{\phi}^{2\mu_1}$ will be allowed. Its descendant $\vec{J}_{-1} \cdot \vec{\phi}^{2\mu_1}$ will compete with the operator $(\overrightarrow{J_{-1}J_{-1}})^{\mu_2} \cdot \vec{\phi}^{\mu_2}$. The former becomes the leading irrelevant operator since its scaling dimension satisfies $\Delta_1^{2\mu_1} < \Delta_2^{\mu_2}$ where

$$\Delta_1^{2\mu_1} = 1 + \Delta_0^{2\mu_1} = 1 + \frac{k+1}{N+k+1}, \qquad (42)$$

$$\Delta_2^{\mu_2} = 2 + \Delta_0^{\mu_2} = 2 + \frac{k}{N+k+1}. \qquad (43)$$

Depending on the fusion rule, the conductance correction will exhibit a non-Fermi liquid behavior, $T^{\Delta_0^{2\mu_1}}$ or $T^{2\Delta_0^{2\mu_1}}$, similar to Eq. (35).

VI. CONCLUSIONS

In this paper, we demonstrated the instability of the strong coupling fixed point in the $\mathrm{SO}(M)$ topological Kondo model, demonstrating the existence of the intermediate coupling fixed point. By developing the generalized Affleck-Ludwig conformal field theory technique, we extended the concept of overscreening to higher rank Lie groups, finding a set of inequalities for the impurity representation, see Eq. (12). We also clarified the conductance correction of the multichannel topological Kondo model, showing that a first order correction given by the LIO exists in the multichannel model but not for single channel. Similarly, in the N-channel charge-Kondo model, the first-order correction exits for $N \geq 3$ but not for $N = 2$ [8] because the fusion rule of two J^ds, spin-1s, gives only spin-0 at $N = 2$. The method of determining the LIO can be applied to other compact Lie groups as we have shown with $\mathrm{Sp}(2k)$. The analysis for getting the $\mathrm{Sp}(2k)$ conductance correction, Eq. (41), is also useful if the spin-1/2 2-flavor Kondo model in Ref. [48, 49] is further generalized to a spin-1/2 k-flavor Kondo model, which is a possible regime for a similar spin-kCK quantum dot device. In addition to the charge conductance, calculating the heat conductance [74] of multichannel topological Kondo model is also feasible based on the methods in our paper.

VII. ACKNOWLEDGEMENTS

[1] J. Kondo, Resistance minimum in dilute magnetic alloys, Progress of theoretical physics **32**, 37 (1964).

[2] Nozières, Ph. and Blandin, A., Kondo effect in real metals, J. Phys. France **41**, 193 (1980).

[3] D. Goldhaber-Gordon, H. Shtrikman, D. Mahalu, D. Abusch-Magder, U. Meirav, and M. A. Kastner, Kondo effect in a single-electron transistor, Nature **391**, 156 (1998).

[4] M. Pustilnik and L. Glazman, Kondo effect in quantum dots, Journal of Physics: Condensed Matter **16**, R513 (2004).

[5] R. M. Potok, I. G. Rau, H. Shtrikman, Y. Oreg, and D. Goldhaber-Gordon, Observation of the two-channel Kondo effect, Nature (London) **446**, 167 (2007).

[6] A. J. Keller, L. Peeters, C. P. Moca, I. Weymann, D. Mahalu, V. Umansky, G. Zaránd, and D. Goldhaber-Gordon, Universal Fermi liquid crossover and quantum criticality in a mesoscopic system, Nature (London) **526**, 237 (2015).

[7] Z. Iftikhar, S. Jezouin, A. Anthore, U. Gennser, F. D. Parmentier, A. Cavanna, and F. Pierre, Two-channel Kondo effect and renormalization flow with macroscopic quantum charge states, Nature (London) **526**, 233 (2015).

[8] Z. Iftikhar, A. Anthore, A. K. Mitchell, F. D. Parmentier, U. Gennser, A. Ouerghi, A. Cavanna, C. Mora, P. Simon, and

F. Pierre, Tunable quantum criticality and super-ballistic transport in a "charge" Kondo circuit, Science **360**, 1315 (2018).

[9] W. Pouse, L. Peeters, C. L. Hsueh, U. Gennser, A. Cavanna, M. A. Kastner, A. K. Mitchell, and D. Goldhaber-Gordon, Quantum simulation of an exotic quantum critical point in a two-site charge Kondo circuit, Nature Physics **19**, 492 (2023).

[10] I. Affleck, Conformal field theory approach to the kondo effect, Acta Phys. Polon. **B26**, 1869 (1995).

[11] P. L. S. Lopes, I. Affleck, and E. Sela, Anyons in multichannel kondo systems, Phys. Rev. B **101**, 085141 (2020).

[12] Y. Komijani, Isolating kondo anyons for topological quantum computation, Phys. Rev. B **101**, 235131 (2020).

[13] D. Gabay, C. Han, P. L. S. Lopes, I. Affleck, and E. Sela, Multi-impurity chiral kondo model: Correlation functions and anyon fusion rules, Phys. Rev. B **105**, 035151 (2022).

[14] M. Lotem, E. Sela, and M. Goldstein, Manipulating non-abelian anyons in a chiral multichannel kondo model, Phys. Rev. Lett. **129**, 227703 (2022).

[15] T. Ren, E. J. König, and A. M. Tsvelik, Topological quantum computation on a chiral kondo chain, Phys. Rev. B **109**, 075145 (2024).

[16] J. Gan, N. Andrei, and P. Coleman, Perturbative approach to the non-Fermi-liquid fixed point of the overscreened Kondo problem, Phys. Rev. Lett. **70**, 686 (1993).

[17] N. Andrei and C. Destri, Solution of the multichannel kondo problem, Phys. Rev. Lett. **52**, 364 (1984).

[18] A. Tsvelick and P. Wiegmann, Exact solution of the multichannel kondo problem, scaling, and integrability, Journal of Statistical Physics **38**, 125 (1985).

[19] V. J. Emery and S. Kivelson, Mapping of the two-channel kondo problem to a resonant-level model, Phys. Rev. B **46**, 10812 (1992).

[20] A. M. Sengupta and A. Georges, Emery-Kivelson solution of the two-channel Kondo problem, Phys. Rev. B **49**, 10020 (1994), arXiv:cond-mat/9312016 [cond-mat].

[21] P. Coleman, L. B. Ioffe, and A. M. Tsvelik, Simple formulation of the two-channel kondo model, Physical Review B **52**, 6611 (1995).

[22] A. V. Rozhkov, Impurity entropy for the two-channel kondo model, International Journal of Modern Physics B **12**, 3457 (1998).

[23] N. Hartman, C. Olsen, S. Lüscher, M. Samani, S. Fallahi, G. C. Gardner, M. Manfra, and J. Folk, Direct entropy measurement in a mesoscopic quantum system, Nature Physics **14**, 1083–1086 (2018).

[24] T. Child, O. Sheekey, S. Lüscher, S. Fallahi, G. C. Gardner, M. Manfra, A. Mitchell, E. Sela, Y. Kleeorin, Y. Meir, and J. Folk, Entropy measurement of a strongly coupled quantum dot, Phys. Rev. Lett. **129**, 227702 (2022).

[25] C. Han, Z. Iftikhar, Y. Kleeorin, A. Anthore, F. Pierre, Y. Meir, A. K. Mitchell, and E. Sela, Fractional entropy of multichannel kondo systems from conductance-charge relations, Phys. Rev. Lett. **128**, 146803 (2022).

[26] I. Affleck and A. W. W. Ludwig, Universal noninteger "ground-state degeneracy" in critical quantum systems, Phys. Rev. Lett. **67**, 161 (1991).

[27] I. Affleck, A current algebra approach to the kondo effect, Nuclear Physics B **336**, 517 (1990).

[28] I. Affleck and A. W. Ludwig, The kondo effect, conformal field theory and fusion rules, Nuclear Physics B **352**, 849 (1991).

[29] I. Affleck and A. W. Ludwig, Critical theory of overscreened kondo fixed points, Nuclear Physics B **360**, 641 (1991).

[30] I. Affleck and A. W. W. Ludwig, Exact conformal-field-theory results on the multichannel kondo effect: Single-fermion green's function, self-energy, and resistivity, Phys. Rev. B **48**, 7297 (1993).

[31] A. W. Ludwig and I. Affleck, Exact conformal-field-theory results on the multi-channel kondo effect: Asymptotic three-dimensional space-and time-dependent multi-point and many-particle green's functions, Nuclear Physics B **428**, 545 (1994).

[32] A. W. W. Ludwig and I. Affleck, Exact, asymptotic, three-dimensional, space- and time-dependent, green's functions in the multichannel kondo effect, Phys. Rev. Lett. **67**, 3160 (1991).

[33] O. Parcollet, A. Georges, G. Kotliar, and A. Sengupta, Over-screened multichannel $SU(N)$ Kondo model: Large-N solution and conformal field theory, Phys. Rev. B **58**, 3794 (1998).

[34] T. Kimura, Abcd of kondo effect, Journal of the Physical Society of Japan **90**, 024708 (2021).

[35] B. Béri and N. R. Cooper, Topological kondo effect with majorana fermions, Phys. Rev. Lett. **109**, 156803 (2012).

[36] B. Béri, Majorana-klein hybridization in topological superconductor junctions, Phys. Rev. Lett. **110**, 216803 (2013).

[37] G. Li, Y. Oreg, and J. I. Väyrynen, Multichannel topological kondo effect, Phys. Rev. Lett. **130**, 066302 (2023).

[38] S. Bollmann, J. I. Väyrynen, and E. J. König, Topological kondo effect with spinful majorana fermions, Phys. Rev. B **110**, 035136 (2024).

[39] F. Buccheri, G. D. Bruce, A. Trombettoni, D. Cassettari, H. Babujian, V. E. Korepin, and P. Sodano, Holographic optical traps for atom-based topological kondo devices, New Journal of Physics **18**, 075012 (2016).

[40] G. Li, E. J. König, and J. I. Väyrynen, Topological symplectic kondo effect, Phys. Rev. B **107**, L201401 (2023).

[41] E. J. König and A. M. Tsvelik, Exact solution of the topological symplectic kondo problem, Annals of Physics **456**, 169231 (2023).

[42] M. Lotem, S. Sankar, T. Ren, M. Goldstein, E. J. König, A. Weichselbaum, E. Sela, and A. M. Tsvelik, Relevance of anisotropy in the kondo effect: Lessons from the symplectic case, Phys. Rev. B **110**, 235122 (2024).

[43] J. I. Väyrynen, A. E. Feiguin, and R. M. Lutchyn, Signatures of topological ground state degeneracy in majorana islands, Phys. Rev. Research **2**, 043228 (2020).

[44] Z. qiang Bao and F. Zhang, Quantum hall charge kondo criticality (2017), arXiv:1708.09139 [cond-mat.str-el].

[45] A. W. Ludwig, Field theory approach to critical quantum impurity problems and applications to the multi-channel kondo effect, International Journal of Modern Physics B **8**, 347 (1994).

[46] M. Lotem, S. Sankar, T. Ren, M. Goldstein, E. J. König, A. Weichselbaum, E. Sela, and A. M. Tsvelik, Relevance of anisotropy in the kondo effect: Lessons from the symplectic case, Phys. Rev. B **110**, 235122 (2024).

[47] A. Tsvelik, Topological kondo effect in star junctions of ising magnetic chains: exact solution, New Journal of Physics **16**, 033003 (2014).

[48] A. K. Mitchell, A. Liberman, E. Sela, and I. Affleck, SO(5) Non-Fermi Liquid in a Coulomb Box Device, Phys. Rev. Lett. **126**, 147702 (2021).

[49] A. Liberman, A. K. Mitchell, I. Affleck, and E. Sela, SO(5) critical point in a spin-flavor Kondo device: Bosonization and refermionization solution, Phys. Rev. B **103**, 195131 (2021).

[50] H. Georgi, *Lie algebras in particle physics: from isospin to unified theories* (Taylor & Francis, 2000).

[51] Z.-Q. Ma, *Group theory for physicists* (World Scientific, 2007).

[52] A. Zee, *Group theory in a nutshell for physicists*, Vol. 17 (Princeton University Press, 2016).

[53] R. Feger, T. W. Kephart, and R. J. Saskowski, Lieart 2.0 – a mathematica application for lie algebras and representation the-

ory, Computer Physics Communications **257**, 107490 (2020).

[54] M. Fabrizio and A. O. Gogolin, Toulouse limit for the over-screened four-channel kondo problem, Phys. Rev. B **50**, 17732 (1994).

[55] A. M. Sengupta and Y. B. Kim, Overscreened single-channel kondo problem, Phys. Rev. B **54**, 14918 (1996).

[56] A. Altland, B. Béri, R. Egger, and A. M. Tsvelik, Multichannel kondo impurity dynamics in a majorana device, Phys. Rev. Lett. **113**, 076401 (2014).

[57] E. Verlinde, Fusion rules and modular transformations in 2d conformal field theory, Nuclear Physics B **300**, 360 (1988).

[58] L.-Y. Hung, Y.-S. Wu, and Y. Zhou, Linking entanglement and discrete anomaly, Journal of High Energy Physics **2018**, 8 (2018).

[59] L. Kong and Z.-H. Zhang, An invitation to topological orders and category theory (2022), arXiv:2205.05565 [cond-mat.str-el].

[60] T. Kimura, Abcd of kondo effect, Journal of the Physical Society of Japan **90**, 024708 (2021).

[61] A. Altland, B. Béri, R. Egger, and A. M. Tsvelik, Bethe ansatz solution of the topological kondo model, Journal of Physics A: Mathematical and Theoretical **47**, 265001 (2014).

[62] A. O. Gogolin, A. A. Nersesyan, and A. M. Tsvelik, *Bosonization and strongly correlated systems* (Cambridge university press, 2004).

[63] A. W. W. LUDWIG, Methods of conformal field theory in condensed matter physics, in *Low-Dimensional Quantum Field Theories for Condensed Matter Physicists* (1995) pp. 389–455.

[64] P. Francesco, P. Mathieu, and D. Sénéchal, *Conformal field theory* (Springer Science & Business Media, 2012).

[65] F. Buccheri, H. Babujian, V. E. Korepin, P. Sodano, and A. Trombettoni, Thermodynamics of the topological kondo

model, Nuclear Physics B **896**, 52 (2015).

[66] K. Michaeli, L. A. Landau, E. Sela, and L. Fu, Electron teleportation and statistical transmutation in multiterminal majorana islands, Phys. Rev. B **96**, 205403 (2017).

[67] A. Rahmani, C.-Y. Hou, A. Feiguin, C. Chamon, and I. Affleck, How to find conductance tensors of quantum multiwire junctions through static calculations: Application to an interacting y junction, Phys. Rev. Lett. **105**, 226803 (2010).

[68] A. Rahmani, C.-Y. Hou, A. Feiguin, M. Oshikawa, C. Chamon, and I. Affleck, General method for calculating the universal conductance of strongly correlated junctions of multiple quantum wires, Phys. Rev. B **85**, 045120 (2012).

[69] See the supplementary material of Ref. [40] for similar calculations in full detail.

[70] M. R. Galpin, A. K. Mitchell, J. Temaismithi, D. E. Logan, B. Béri, and N. R. Cooper, Conductance fingerprint of majorana fermions in the topological kondo effect, Phys. Rev. B **89**, 045143 (2014).

[71] L. Herviou, K. Le Hur, and C. Mora, Many-terminal majorana island: From topological to multichannel kondo model, Phys. Rev. B **94**, 235102 (2016).

[72] T. Kimura and S. Ozaki, Fermi/non-fermi mixing in su(n) kondo effect, Journal of the Physical Society of Japan **86**, 084703 (2017).

[73] M. Oshikawa, C. Chamon, and I. Affleck, Junctions of three quantum wires, Journal of Statistical Mechanics: Theory and Experiment **2006**, P02008 (2006).

[74] F. Buccheri, A. Nava, R. Egger, P. Sodano, and D. Giuliano, Violation of the wiedemann-franz law in the topological kondo model, Phys. Rev. B **105**, L081403 (2022).

Appendix A: SO($2m$) Lie algebra and spinor representation

In this section, we introduce the basics of the SO($2m$) Lie algebra and show that the ground states of the SO($2m$) topological Kondo interaction (no kinetic energy) are at half-filling (the m-particle sector).

1. SO($2m$) Lie algebra

The group SO($2m$) is generated by $m(2m-1)$ generators. In our case, they can be Majorana bilinears $-\mathrm{i}\gamma_\alpha\gamma_\beta/2$ with $\alpha < \beta$. The rank of $\mathfrak{so}(2m)$ Lie algebra is m, which means that we have m Cartan generators. The corresponding Cartan generators and the $2m(m-1)$ roots are [50, 52]

$$H_i = -\mathrm{i}\gamma_{2i-1}\gamma_{2i}/2, \quad E_{ij}^{ss'} = -\mathrm{i}(\gamma_{2i-1} + \mathrm{i}s\gamma_{2i})(\gamma_{2j-1} + \mathrm{i}s'\gamma_{2j})/4 \tag{A1}$$

where $i < j = 1, 2, \ldots, m$ and $s, s' = \pm 1$. We can check the commutation relations are

$$[H_j, E_{jk}^{ss'}] = sE_{jk}^{ss'}, \quad [H_k, E_{jk}^{ss'}] = s'E_{jk}^{ss'}. \tag{A2}$$

Other H_is with $i \neq j, k$ will commute with $E_{jk}^{ss'}$. From above, we obtain the simple roots, which are

$$\alpha_1 = (1, -1, 0, \ldots, 0), \tag{A3}$$

$$\alpha_2 = (0, 1, -1, 0, \ldots, 0), \ldots, \tag{A4}$$

$$\alpha_{m-1} = (0, \ldots, 0, 1, -1), \tag{A5}$$

$$\alpha_m = (0, \ldots, 0, 1, 1). \tag{A6}$$

Cartan matrix is defined as $C_{ij} = 2(\alpha_i \cdot \alpha_j)/(\alpha_i \cdot \alpha_i)$. The fundamental weights are

$$\mu_1 = (1, 0, \ldots, 0), \tag{A7}$$
$$\mu_2 = (1, 1, 0, \ldots, 0), \ldots, \tag{A8}$$
$$\mu_{m-2} = (1, \ldots, 1, 0, 0), \tag{A9}$$
$$\mu_{m-1} = (1, \ldots, 1, -1)/2, \tag{A10}$$
$$\mu_m = (1, \ldots, 1)/2. \tag{A11}$$

Any representation can be written as $\mu = \sum_{i=1}^m a_i \mu_i$ where a_is are Dynkin's labels. The corresponding Casimir invariant for this representation μ is given by [51]

$$c(R) = \sum_{i,j=1}^m (\alpha_i \cdot \alpha_i)(a_i/2 + 1)(C^{-1})_{ij} a_j. \tag{A12}$$

2. Representation of S^A, J^A and decomposition of $R(S^A) \otimes R(J^A)$

The spinor representations S^A using Majorana operators can be further written in terms of Pauli matrices σ_i, $i = 1, 2, 3$:

$$\gamma_1 = \sigma_1 \otimes \sigma_3 \otimes \cdots \otimes \sigma_3, \ \gamma_2 = \sigma_2 \otimes \sigma_3 \otimes \cdots \otimes \sigma_3,$$
$$\gamma_3 = \mathbb{I} \otimes \sigma_1 \otimes \sigma_3 \otimes \cdots \otimes \sigma_3, \ \gamma_4 = \mathbb{I} \otimes \sigma_2 \otimes \sigma_3 \otimes \cdots \otimes \sigma_3, \ \ldots,$$
$$\gamma_{2m-1} = \mathbb{I} \otimes \cdots \otimes \mathbb{I} \otimes \sigma_1, \ \gamma_{2m} = \mathbb{I} \otimes \cdots \otimes \mathbb{I} \otimes \sigma_2. \tag{A13}$$

The natural basis for the above m spin-1/2 operators is the spin-$\uparrow, \downarrow$ states. Then, the Cartan generators measure the z-component of each spin because $H_i \sim \sigma_3^{(i)}$. The root $E_{jk}^{ss'}$ is nearly $\sigma_s^{(j)} \sigma_{s'}^{(k)}$ where $\sigma_s = \sigma_1 + i s \sigma_2$. Representations are defined through their highest weights. We can easily find that the highest weights of this spinor representation are $|\uparrow \ldots \uparrow\uparrow\rangle$ and $|\uparrow \ldots \uparrow\downarrow\rangle$. These two highest-weight states are eigenstates of Cartan generators, and the eigenvalues are μ_{m-1} [Eq. (A10)] and μ_m [Eq. (A11)], which gives Eq. (7): $R(S^A) = (\mu_m) \oplus (\mu_{m-1})$ in the main text. The difference between the (μ_{m-1}) and (μ_m) subspaces is their parities, which can be measured by $(-1)^m \prod_{i=1}^{2m} \gamma_i = \sigma_3 \otimes \cdots \otimes \sigma_3$. They are both 2^{m-1}-dimensional.

When it comes to the representations of J^A, we need to consider the particle sectors separately. The dimension of the K-particle sector is equal to the dimension of the linear space in which the states live. As we defined in Sec. II, the number of states that live in the K-particle sector is $\binom{2m}{K}$. The total dimension for J^A is thus the sum of the dimensions of all K-particle sectors $\sum_{i=0}^{2m} \binom{2m}{K} = 2^{2m}$, which verifies our conclusion that the representation of J^A is the same as the representation given by $R(S^A) \otimes R(S^A)$ [Eq. (3)] in terms of its dimensions. We can decompose $R(J^A) = R(S^A) \otimes R(S^A)$ as $\bigoplus_{i=0}^{2m} R(J_n^{A,i})$ with

$$R(J^{A,i}) = R(J^{A,2m-i}) = (\mu_i) \text{ for } 0 \le i \le m - 2; \tag{A14}$$
$$R(J^{A,m-1}) = (\mu_{m-1} + \mu_m); \ \ R(J^{A,m}) = (2\mu_{m-1}) \oplus (2\mu_m). \tag{A15}$$

We used the following three decomposition rules:

$$(\mu_{m-1}) \otimes (\mu_{m-1}) = (2\mu_{m-1}) \bigoplus_{i=1}^{[m/2]} (\mu_{m-2i}); \ \ (\mu_m) \otimes (\mu_m) = (2\mu_m) \bigoplus_{i=1}^{[m/2]} (\mu_{m-2i}); \tag{A16}$$
$$(\mu_{m-1}) \otimes (\mu_m) = (\mu_{m-1} + \mu_m) \bigoplus_{j=1}^{[(m-1)/2]} (\mu_{m-2j-1}). \tag{A17}$$

Note that $\mu_0 = \mathbf{0}$ and the above equations are symmetric for μ_{m-1} and μ_m. We can verify using LieART [53] that $R(S^A) \otimes R(J^{A,K})$ contains $(\mu_m) \oplus (\mu_{m-1})$ for every $0 \le K \le 2m$. The representation μ_{m-1} and μ_m have the smallest Casimir invariant according to Eq. (A12). Thus, the lowest Kondo energy [Eq. (4)] is at $K = m$ (half-filling), which maximizes $c[R(J_n^{A,K})] = K(2m - K)$ [see also Eq. (8)].

Appendix B: Effective Hamiltonian of SO(4) topological Kondo at strong coupling

In this section, we calculate the ground states of the SO(4) topological Kondo interaction and find the strong coupling effective Hamiltonian of it, i.e., Eq. (B53).

1. Ground states of the SO(4) topological Kondo interaction

The simple roots and fundamental weights of SO(4) are [50, 52]

$$\alpha_1 = (1, -1),\ \alpha_2 = (1, 1);\ \mu_1 = (1/2, -1/2),\ \mu_2 = (1/2, 1/2). \tag{B1}$$

The Casimir invariant is thus

$$c(a_1\mu_1 + a_2\mu_2) = \frac{1}{2}a_1(a_2 + 2) + \frac{1}{2}a_1(a_2 + 2). \tag{B2}$$

The representation $R(S^A) = (\mu_1) \oplus (\mu_2)$ gives that $c(R(S^A)) = 3/2$ which agrees with Eq. (6). The dimension of the K-particle sector $R(J^{A,K})$ is $\binom{4}{K}$. The corresponding representations $R(J^A) = R(S^A) \otimes R(S^A) = [(\mu_1) \oplus (\mu_2)] \otimes [(\mu_1) \oplus (\mu_2)]$ can be written as $\bigoplus_{K=0}^{4} R(J^{A,K})$ where

$$R(J_n^{A,0}) = R(J_n^{A,4}) = (\mathbf{0}),\ R(J_n^{A,1}) = R(J_n^{A,3}) = (\mu_1 + \mu_2) \text{ and } R(J_n^{A,2}) = (2\mu_1) \oplus (2\mu_2). \tag{B3}$$

Here, we used a fact that $(\mu_1) \otimes (\mu_1) = (\mathbf{0}) \oplus (2\mu_1)$, $(\mu_2) \otimes (\mu_2) = (\mathbf{0}) \oplus (2\mu_2)$ and $(\mu_1) \otimes (\mu_2) = (\mu_1 + \mu_2)$. We can check that $c(R(J_n^{A,K})) = K(4 - K)$ which agrees with Eq. (8). The decompositions of $R(S^A) \otimes R(J^A) = \bigoplus_{K=0}^{4} R(S^A) \otimes R(J^{A,K})$ where

$$R(S^A) \otimes R(J^{A,0,4}) = [(\mu_1) \oplus (\mu_2)] \otimes (\mathbf{0}) = (\mu_1) \oplus (\mu_2), \tag{B4}$$

$$R(S^A) \otimes R(J_n^{A,1,3}) = [(\mu_1) \oplus (\mu_2)] \otimes (\mu_1 + \mu_2) = (\mu2) \oplus (2\mu_1 + \mu_2) \oplus (\mu_1 + 2\mu_2) \oplus (\mu_1), \tag{B5}$$

$$R(S^A) \otimes R(J_n^{A,2}) = [(\mu_1) \oplus (\mu_2)] \otimes [(2\mu_1) \otimes (2\mu_2)] = (\mu_1) \oplus (3\mu_1) \oplus (\mu_1 + 2\mu_2) \oplus (2\mu_1 + \mu_2) \oplus (3\mu_2) \oplus (\mu_2). \tag{B6}$$

The above expansions verify our conclusion that $(\mu_1) \oplus (\mu_2)$ always exists in $R(S^A) \otimes R(J^{A,K})$ for every K. The Kondo energy Eq. (4) for SO(4) is

$$E_{\text{Kondo}} = \frac{1}{2}\Big\{c[R(S^A) \otimes R(J^{A,K})] - c[R(S^A)] - c[R(J^{A,K})]\Big\} \tag{B7}$$

$$= \frac{1}{2}\Big\{c[R(S^A) \otimes R(J^{A,K})] - \frac{M(M-1)}{8} - K(4-K)\Big\}. \tag{B8}$$

The nontrivial minima of $c(a_1\mu_1 + a_2\mu_2)$ when $a_{1,2}$ are both nonnegative integers are given by $(a_1, a_2) = (1, 0)$ or $(0, 1)$, i.e. μ_1 or μ_2, which is contained in any $R(S^A) \otimes R(J_n^{A,K})$. Thus, we conclude that the lowest SO(4) Kondo energy is at $K = 2$ where it maximizes the $c(R(J^{A,K})) = K(4 - K)$.

It is knowm that SO(4) $\sim$ SU(2) $\times$ SU(2) which can be seen from Eq. (B2) where the Casimir invariant of SO(4) can be reformulated as $c(a_1\mu_1 + a_2\mu_2) = 2[s_1(s_1 + 1)] + 2[s_2(s_2 + 1)]$ for spin-$s_{1,2} = a_{1,2}/2$. Based on the fact that $(\mu_1) \otimes (\mu_1) = (\mathbf{0}) \oplus (2\mu_1)$, $(\mu_2) \otimes (\mu_2) = (\mathbf{0}) \oplus (2\mu_2)$ and $(\mu_1) \otimes (\mu_2) = (\mu_1 + \mu_2)$, one can consider the above decomposition as the decomposition for two independent spins. Furthermore, the conduction electrons are two independent spin-1 particles for the lowest energy case $J^{A,2}$ which is $(2\mu_1) \oplus (2\mu_2)$. The lowest energy in this 2-particle sector is (μ_1) and (μ_2) given by $(\mu_1) \otimes (2\mu_1) = (\mu_1) \oplus (3\mu_1)$ and $(\mu_2) \otimes (2\mu_2) = (\mu_2) \oplus (3\mu_2)$. In the language of SU(2) spin decompositions, they are $1/2 \otimes 1 = 1/2 \oplus 3/2$, which is the same decomposition used for getting the ground state of the 2-channel SU(2) Kondo model at the strong coupling and also half-filling.

2. Representations and strong coupling solutions

The Casimir invariant $c(a_1, a_2)$ for a representation of generators R^A labeled by $a_1\mu_1 + a_2\mu_2$ is given by Eq. (B2), which gives $\sum_A(R^A)^2 = c\,\mathbb{I}_{\dim \times \dim}$. The $K = 0, 4$-particle sector contain only one state $|0\rangle$ or $|\text{full}\rangle = \psi_1^\dagger\psi_2^\dagger\psi_3^\dagger\psi_4^\dagger|0\rangle$ for electrons. This leads to $J^{A,0} = \langle 0|J^A|0\rangle = 0$ and $H_K = 0$. For the 1, 3-particle sector, we get $J^{A,K=1,3} = T^A$ and the representation is $\mu_1 + \mu_2$, a 4 dimensional representation with $\sum_A(T^A)^2 = 3\,\mathbb{I}_{4\times 4}$. Next, we define the 2-particle states as $|a\rangle = \sum_{ij}(B^a)_{ij}\psi_i^\dagger\psi_j^\dagger|0\rangle$ with $a = 1, \ldots, 6$, $(B^a)^T = -B^a$ and $(B^a)^\dagger = B^a$. Normalization of state $|a\rangle$ requires $2\,\text{Tr}(B^a B^b) = \delta^{ab}$. Thus, the 2-particle matrix representation for the generator J^A is

$$[J^{A,K=2}]_{ba} = \langle b|J^A|a\rangle = \sum_{ii'jj'\rho\sigma}(B^b)_{i'j'}^*(T^A)_{\rho\sigma}(B^a)_{ij}\langle 0|\psi_{j'}\psi_{i'}\psi_\rho^\dagger\psi_\sigma\psi_i^\dagger\psi_j^\dagger|0\rangle = 4\,\text{Tr}(B^b T^A B^a). \tag{B9}$$

Let us consider the following B tensor

$$[B^{b=(b_1,b_2)}]_{ij} = -\frac{i}{2!}\delta_i^{b_1}\delta_j^{b_2} + \frac{i}{2!}\delta_j^{b_1}\delta_i^{b_2} \text{ with } b_1 < b_2. \tag{B10}$$

Here, $b_1, b_2, i, j = 1, 2, 3, 4$. This six-dimensional space spanned by $|a\rangle$ is reducible and the representation is $2\mu_1 \oplus 2\mu_2$ because we checked that $\sum_A [J^{A,K=2}]^2 = 4\mathbb{I}_{6\times 6}$. Each of these two representations is three-dimensional.

After figuring out the representations of K-particle J^A, we show the decompositions for each $J^{A,K}$ with S^A ($\mu_1 \oplus \mu_2$) in the following: H_K:

$$R(S^A) \otimes R(J^{A,K=1,3}) = (\mu_1 \oplus \mu_2) \otimes (\mu_1 + \mu_2) = \mu_2 \oplus (2\mu_1 + \mu_2) \oplus (\mu_1 + 2\mu_2) \oplus \mu_1; \tag{B11}$$

$$R(S^A) \otimes R(J^{A,K=2}) = (\mu_1 \oplus \mu_2) \otimes (2\mu_1 \oplus 2\mu_2) = \mu_1 \oplus 3\mu_1 \oplus (\mu_1 + 2\mu_2) \oplus (2\mu_1 + \mu_2) \oplus 3\mu_2 \oplus \mu_2, \tag{B12}$$

where we used the following decomposition rules

$$\mu_1 \otimes \mu_1 = \mathbf{0} \oplus 2\mu_1; \ \mu_2 \otimes \mu_2 = \mathbf{0} \oplus 2\mu_2; \ \mu_1 \otimes \mu_2 = \mu_1 + \mu_2. \tag{B13}$$

We include all the results in the following table.

K	$(\mu_1 \oplus \mu_2) \otimes (\mu_1 + \mu_2)$ (4×4)	$\sum_A (S^A + J^{A,K=1,3})^2$	$-\sum_A (S^A)^2$	$-\sum_A (J^{A,K=1,3})^2$	$2H_K/\lambda$
$1,3$	$2\mu_1 + \mu_2$ (6)	$11/2$	$-3/2$	-3	1
$1,3$	$\mu_1 + 2\mu_2$ (6)	$11/2$	$-3/2$	-3	1
$1,3$	μ_2 (2)	$3/2$	$-3/2$	-3	-3
$1,3$	μ_1 (2)	$3/2$	$-3/2$	-3	-3

TABLE III. 1,3-particle decomposition with dimension and energy. The numbers near the representations are dimensions.

K	$(\mu_1 \oplus \mu_2) \otimes (2\mu_1 \oplus 2\mu_2)$ (4×6)	$\sum_A (S^A + J^{A,K=2})^2$	$-\sum_A (S^A)^2$	$-\sum_A (J^{A,K=2})^2$	$2H_K/\lambda$
2	$3\mu_1$ (4)	$15/2$	$-3/2$	-4	2
2	$3\mu_2$ (4)	$15/2$	$-3/2$	-4	2
2	$\mu_1 + 2\mu_2$ (6)	$11/2$	$-3/2$	-4	0
2	$2\mu_1 + \mu_2$ (6)	$11/2$	$-3/2$	-4	0
2	μ_1 (2)	$3/2$	$-3/2$	-4	-4
2	μ_2 (2)	$3/2$	$-3/2$	-4	-4

TABLE IV. 2-particle decomposition with dimension and energy. The numbers near the representations are dimensions.

We conclude that the ground states are represented by μ_1 and μ_2 at 2-particle sector (half-filling). Also, the above energies have two copies because μ_1 and μ_2 are interchangeable.

3. Eigenstates

Next, we define the eigenstates of H_K in $1, 2, 3$-particle sector. At 1-particle sector, the general form for the states are

$$|K = 1, \alpha\rangle = \sum_{ij}(t^\alpha)_{ij}|i\rangle \otimes \psi_j^\dagger |0\rangle, \ i, j = 1, \ldots, 4; \ \alpha = 1, \ldots 16. \tag{B14}$$

Based on the above decomposition, we define that

$$(2H_K/\lambda)|K = 1, \alpha = 1, \ldots, 12\rangle = |K = 1, \alpha = 1, \ldots, 12\rangle; \tag{B15}$$

$$(2H_K/\lambda)|K = 1, \alpha = 13, \ldots, 16\rangle = -3|K = 1, \alpha = 13, \ldots, 16\rangle. \tag{B16}$$

Similarly, at 2-particle, we define

$$|K = 2, \beta\rangle = \sum_{ia}(r^\beta)_{ia}|i\rangle \otimes |a\rangle = \sum_{ia}(r^\beta)_{ia}|i\rangle \otimes \sum_{kl}(B^a)_{kl}\psi_k^\dagger \psi_l^\dagger |0\rangle, \ i, k, l = 1, \ldots, 4; \ a = 1, \ldots, 6; \ \beta = 1, \ldots, 24, \tag{B17}$$

and

$$(2H_K/\lambda)|K = 2, \beta = 1, \ldots, 8\rangle = 2|K = 2, \beta = 1, \ldots, 8\rangle; \tag{B18}$$

$$(2H_K/\lambda)|K = 2, \beta = 9, \ldots, 20\rangle = 0; \tag{B19}$$

$$(2H_K/\lambda)|K = 2, \beta = 21, \ldots, 24\rangle = -4|K = 2, \beta = 21, \ldots, 24\rangle. \tag{B20}$$

At 3-particle, we define

$$|K = 3, \alpha'\rangle = \sum_{ij} (t'^{\alpha'})_{ij}|i\rangle \otimes \psi_j|\text{full}\rangle, \quad i, j = 1, \ldots, 4; \ \alpha' = 1, \ldots 16. \tag{B21}$$

Under the electrons states $\psi_j|\text{full}\rangle$, $J^{(3),A} = J^{(1),A} = T^A$, which means that $t' = t$. Thus,

$$(2H_K/\lambda)|K = 3, \alpha = 1, \ldots, 12\rangle = |K = 2, \alpha = 1, \ldots, 12\rangle; \tag{B22}$$

$$(2H_K/\lambda)|K = 3, \alpha = 13, \ldots, 16\rangle = -3|K = 2, \alpha = 13, \ldots, 16\rangle. \tag{B23}$$

4. Perturbative inclusion of the leads

The lead fermion is $\psi_{s,i}$ where s labels the site and $i = 1, \ldots 4$ labels the flavor. The nearest site to the impurity is at $s = 1$ and we ignored this $s = 1$ on the above nearest lead fermion. But now we include the hopping energy between the first site and the second site $H_{12} = -g\sum_p(\psi_{1,p}^\dagger\psi_{2,p} + \psi_{2,p}^\dagger\psi_{1,p})$:

$$(H_{\text{eff}})_{ij} = \sum_{\alpha=1}^{12} \frac{\langle K = 2, \beta = 20 + i|H_{12}|K = 1, \alpha\rangle\langle K = 1, \alpha|H_{12}|K = 2, \beta = 20 + j\rangle}{(-2\lambda - \lambda/2)} \tag{B24}$$

$$+ \sum_{\alpha=13}^{16} \frac{\langle K = 2, \beta = 20 + i|H_{12}|K = 1, \alpha\rangle\langle K = 1, \alpha|H_{12}|K = 2, \beta = 20 + j\rangle}{(-2\lambda + 3\lambda/2)} \tag{B25}$$

$$+ \sum_{\alpha=1}^{12} \frac{\langle K = 2, \beta = 20 + i|H_{12}|K = 3, \alpha\rangle\langle K = 3, \alpha|H_{12}|K = 2, \beta = 20 + j\rangle}{(-2\lambda - \lambda/2)} \tag{B26}$$

$$+ \sum_{\alpha=13}^{16} \frac{\langle K = 2, \beta = 20 + i|H_{12}|K = 3, \alpha\rangle\langle K = 3, \alpha|H_{12}|K = 2, \beta = 20 + j\rangle}{(-2\lambda + 3\lambda/2)}. \tag{B27}$$

We need to calculate the following terms:

$$\langle K = 1, \alpha|H_{12}|K = 2, \beta\rangle = -g\sum_p\sum_{i'j'}(t^\alpha)_{i'j'}^*\sum_{ia}(r^\beta)_{ia}\sum_{kl}(B^a)_{kl}\langle i'|i\rangle\langle 0|\psi_{j'}\psi_p\psi_k^\dagger\psi_l^\dagger|0\rangle\psi_{2,p}^\dagger \tag{B28}$$

$$= 2g\sum_p\sum_{ila}(t^\alpha)_{il}^*(r^\beta)_{ia}(B^a)_{lp}\psi_{2,p}^\dagger; \tag{B29}$$

$$\langle K = 2, \beta|H_{12}|K = 1, \alpha\rangle = 2g\sum_p\sum_{ila}(t^\alpha)_{il}(r^\beta)_{ia}^*(B^a)_{lp}^*\psi_{2,p}; \tag{B30}$$

$$\langle K = 3, \alpha|H_{12}|K = 2, \beta\rangle = -g\sum_p\sum_{i'j'}(t^\alpha)_{i'j'}^*\sum_{ia}(r^\beta)_{ia}\sum_{kl}(B^a)_{kl}\langle i'|i\rangle\langle\text{full}|\psi_{j'}^\dagger\psi_p^\dagger\psi_k^\dagger\psi_l^\dagger|0\rangle\psi_{2,p} \tag{B31}$$

$$= -g\sum_p\sum_{ija}(t^\alpha)_{ij}^*(r^\beta)_{ia}\sum_{kl}\epsilon_{jpkl}(B^a)_{kl}\psi_{2,p} = 2g\sum_p\sum_{ija}(t^\alpha)_{ij}^*(r^\beta)_{ia}(C^a)_{jp}\psi_{2,p}; \tag{B32}$$

$$\langle K = 2, \beta|H_{12}|K = 3, \alpha\rangle = 2g\sum_p\sum_{ija}(t^\alpha)_{ij}(r^\beta)_{ia}^*(C^a)_{jp}^*\psi_{2,p}^\dagger \tag{B33}$$

where we define $(C^a)_{jp} = -\frac{1}{2}\sum_{kl}\epsilon_{jpkl}(B^a)_{kl}$. Thus,

$$(H_{\text{eff}})_{11} = -\frac{16g^2}{5\lambda} - \frac{22g^2}{15\lambda}\sum_{pq}(T^{12} + T^{34})_{pq}\psi_{2,p}^\dagger\psi_{2,q}; \ (H_{\text{eff}})_{14} = \frac{22g^2}{15\lambda}\sum_{pq}(T^{13} - T^{24} + iT^{14} + iT^{23})_{pq}\psi_{2,p}^\dagger\psi_{2,q}; \tag{B34}$$

$$(H_{\text{eff}})_{41} = \frac{22g^2}{15\lambda}\sum_{pq}(T^{13} - T^{24} - iT^{14} - iT^{23})_{pq}\psi_{2,p}^\dagger\psi_{2,q}; \ (H_{\text{eff}})_{22} = -\frac{16g^2}{5\lambda} - \frac{22g^2}{15\lambda}\sum_{pq}(T^{12} - T^{34})_{pq}\psi_{2,p}^\dagger\psi_{2,q}; \tag{B35}$$

$$(H_{\text{eff}})_{33} = -\frac{16g^2}{5\lambda} + \frac{22g^2}{15\lambda}\sum_{pq}(T^{12} - T^{34})_{pq}\psi_{2,p}^\dagger\psi_{2,q}; \ (H_{\text{eff}})_{23} = \frac{22g^2}{15\lambda}\sum_{pq}(T^{13} + T^{24} - iT^{14} + iT^{23})_{pq}\psi_{2,p}^\dagger\psi_{2,q}; \quad \text{(B36)}$$

$$(H_{\text{eff}})_{32} = \frac{22g^2}{15\lambda}\sum_{pq}(T^{13} + T^{24} + iT^{14} - iT^{23})_{pq}\psi_{2,p}^\dagger\psi_{2,q}; \ (H_{\text{eff}})_{44} = -\frac{16g^2}{5\lambda} + \frac{22g^2}{15\lambda}\sum_{pq}(T^{12} + T^{34})_{pq}\psi_{2,p}^\dagger\psi_{2,q}. \quad \text{(B37)}$$

Before calculating the whole H_{eff}, we write down all matrix $S^{A=(\alpha,\beta)} = -\frac{i}{2}\gamma_\alpha\gamma_\beta$ according to the definitions Eq. (A13):

$$S^{12} = \begin{pmatrix} \frac{1}{2} & & & \\ & \frac{1}{2} & & \\ & & -\frac{1}{2} & \\ & & & -\frac{1}{2} \end{pmatrix}; \ S^{13} = \begin{pmatrix} & & & -\frac{i}{2} \\ & & \frac{i}{2} & \\ & -\frac{i}{2} & & \\ \frac{i}{2} & & & \end{pmatrix}; \ S^{14} = \begin{pmatrix} & & & -\frac{1}{2} \\ & & -\frac{1}{2} & \\ & -\frac{1}{2} & & \\ -\frac{1}{2} & & & \end{pmatrix}; \quad \text{(B38)}$$

$$S^{23} = \begin{pmatrix} & & -\frac{1}{2} & \\ & & & \frac{1}{2} \\ \frac{1}{2} & & & \\ & -\frac{1}{2} & & \end{pmatrix}; \ S^{24} = \begin{pmatrix} & & \frac{i}{2} & \\ & & & \frac{i}{2} \\ -\frac{i}{2} & & & \\ & -\frac{i}{2} & & \end{pmatrix}; \ S^{34} = \begin{pmatrix} \frac{1}{2} & & & \\ & -\frac{1}{2} & & \\ & & \frac{1}{2} & \\ & & & -\frac{1}{2} \end{pmatrix}. \quad \text{(B39)}$$

Thus,

$$S^{12} + S^{34} = \begin{pmatrix} 1 & & & \\ & 0 & & \\ & & 0 & \\ & & & -1 \end{pmatrix}; \ S^{12} - S^{34} = \begin{pmatrix} 0 & & & \\ & 1 & & \\ & & -1 & \\ & & & 0 \end{pmatrix}; \ \frac{1}{2}(iS^{13} - iS^{24} - S^{14} - S^{23}) = \begin{pmatrix} & & & 1 \\ & 0 & & \\ & & 0 & \\ & & & 0 \end{pmatrix}; \quad \text{(B40)}$$

$$\frac{1}{2}(-iS^{13} - iS^{24} - S^{14} + S^{23}) = \begin{pmatrix} & & 0 & \\ & & & 1 \\ 0 & & & \\ & 0 & & \end{pmatrix}; \ \frac{1}{2}(iS^{13} + iS^{24} - S^{14} + S^{23}) = \begin{pmatrix} & & 0 & \\ & & & 0 \\ 1 & & & \\ & 0 & & \end{pmatrix}; \quad \text{(B41)}$$

$$\frac{1}{2}(-iS^{13} + iS^{24} - S^{14} - S^{23}) = \begin{pmatrix} & 0 & & \\ & & 0 & \\ & & & 0 \\ 1 & & & \end{pmatrix}. \quad \text{(B42)}$$

Finally,

$$H_{\text{eff}} = \begin{pmatrix} 1 & & & \\ & 0 & & \\ & & 0 & \\ & & & 0 \end{pmatrix}(H_{\text{eff}})_{11} + \begin{pmatrix} 0 & & & \\ & 1 & & \\ & & 0 & \\ & & & 0 \end{pmatrix}(H_{\text{eff}})_{22} + \begin{pmatrix} 0 & & & \\ & 0 & & \\ & & 1 & \\ & & & 0 \end{pmatrix}(H_{\text{eff}})_{33} + \begin{pmatrix} 0 & & & \\ & 0 & & \\ & & 0 & \\ & & & 1 \end{pmatrix}(H_{\text{eff}})_{44} \quad \text{(B43)}$$

$$+ (H_{\text{eff}})_{14}\begin{pmatrix} & & & 1 \\ & 0 & & \\ & & 0 & \\ & & & 0 \end{pmatrix} + (H_{\text{eff}})_{23}\begin{pmatrix} & & 0 & \\ & & & 1 \\ 0 & & & \\ & 0 & & \end{pmatrix} + (H_{\text{eff}})_{32}\begin{pmatrix} & & 0 & \\ & & & 0 \\ 1 & & & \\ & 0 & & \end{pmatrix} + (H_{\text{eff}})_{41}\begin{pmatrix} & 0 & & \\ & & 0 & \\ & & & 0 \\ 1 & & & \end{pmatrix} \quad \text{(B44)}$$

$$= -\frac{16g^2}{5\lambda}\mathbb{I}_{4\times4} - \frac{22g^2}{15\lambda}(S^{12} + S^{34})\sum_{pq}(T^{12} + T^{34})_{pq}\psi_{2,p}^\dagger\psi_{2,q} - \frac{22g^2}{15\lambda}(S^{12} - S^{34})\sum_{pq}(T^{12} - T^{34})_{pq}\psi_{2,p}^\dagger\psi_{2,q} \quad \text{(B45)}$$

$$+ \frac{11g^2}{15\lambda}(iS^{13} - iS^{24} - S^{14} - S^{23})\sum_{pq}(T^{13} - T^{24} + iT^{14} + iT^{23})_{pq}\psi_{2,p}^\dagger\psi_{2,q} \quad \text{(B46)}$$

$$+ \frac{11g^2}{15\lambda}(-iS^{13} + iS^{24} - S^{14} - S^{23})\sum_{pq}(T^{13} - T^{24} - iT^{14} - iT^{23})_{pq}\psi_{2,p}^\dagger\psi_{2,q} \quad \text{(B47)}$$

$$+ \frac{11g^2}{15\lambda}(-iS^{13} - iS^{24} - S^{14} + S^{23})\sum_{pq}(T^{13} + T^{24} - iT^{14} + iT^{23})_{pq}\psi_{2,p}^\dagger\psi_{2,q} \quad \text{(B48)}$$

$$+ \frac{11g^2}{15\lambda}(iS^{13} + iS^{24} - S^{14} + S^{23})\sum_{pq}(T^{13} + T^{24} + iT^{14} - iT^{23})_{pq}\psi_{2,p}^\dagger\psi_{2,q} \quad \text{(B49)}$$

$$= -\frac{16g^2}{5\lambda}\mathbb{I}_{4\times4} - \frac{44g^2}{15\lambda}\Big[S^{12}\psi^\dagger T^{12}\psi + S^{34}\psi^\dagger T^{34}\psi + S^{14}\psi^\dagger T^{13}\psi + S^{13}\psi^\dagger T^{14}\psi - S^{24}\psi^\dagger T^{23}\psi - S^{23}\psi^\dagger T^{24}\psi\Big]. \quad \text{(B50)}$$

We can perform the following rotations

$$\exp\left(-\frac{\mathrm{i}\pi}{2}T^{12}\right)T^{13}\exp\left(\frac{\mathrm{i}\pi}{2}T^{12}\right)=T^{23},\ \exp\left(-\frac{\mathrm{i}\pi}{2}T^{12}\right)T^{14}\exp\left(\frac{\mathrm{i}\pi}{2}T^{12}\right)=T^{24}, \tag{B51}$$

$$\exp\left(-\frac{\mathrm{i}\pi}{2}T^{12}\right)T^{23}\exp\left(\frac{\mathrm{i}\pi}{2}T^{12}\right)=-T^{13},\ \exp\left(-\frac{\mathrm{i}\pi}{2}T^{12}\right)T^{24}\exp\left(\frac{\mathrm{i}\pi}{2}T^{12}\right)=-T^{14} \tag{B52}$$

such that

$$H_{\mathrm{eff}}=-\frac{16g^2}{5\lambda}\mathbb{I}_{4\times4}-\frac{44g^2}{15\lambda}\left[S^{12}\psi^\dagger T^{12}\psi+S^{34}\psi^\dagger T^{34}\psi+S^{14}\psi^\dagger T^{23}\psi+S^{13}\psi^\dagger T^{24}\psi+S^{24}\psi^\dagger T^{13}\psi+S^{23}\psi^\dagger T^{14}\psi\right]. \tag{B53}$$

One can interchange the definitions of γ_1,γ_2 and γ_3,γ_4 in S^A such that the second term in Eq. (B53) becomes the $N=1,M=4$ topological Kondo model.

Appendix C: Current algebra of the N-channel topological Kondo model

In this section, we derive the Kac-Moody algebra for the N-channel topological SO(M) Kondo model. The current operator for N-channel topological SO(M) Kondo model is defined as

$$\widetilde{J}^A(x)=\sum_{n=1}^{N}J_n^A=\sum_{n=1}^{N}\sum_{\alpha,\beta}^{M}\psi_{n,\alpha}^\dagger(x)(T^A)_{\alpha\beta}\psi_{n,\beta}(x) \tag{C1}$$

where T^As are the traceless generators of SO(M) group. They are defined as

$$(T^A)_{\alpha\beta}\equiv(T^{rs})_{\alpha\beta}=\mathrm{i}(\delta_\alpha^r\delta_\beta^s-\delta_\beta^r\delta_\alpha^s). \tag{C2}$$

By definition, $1\leq r<s\leq M$. Thus, $A=1,\ldots,M(M-1)/2$. They satisfy $\mathrm{Tr}(T^AT^B)=2\delta^{AB}$ and $[T^A,T^B]=\mathrm{i}\sum_C f^{ABC}T^C$ where $f^{ABC}=(-\mathrm{i}/2)\mathrm{Tr}([T^A,T^B]T^C)$ is the structure constant. We define the normal order with respect to the (zero-temperature) Fermi sea, which means that we move creation (annihilation) operators to the right when this particle exists (does not exist) in the Fermi sea. The normal order of the current operator is

$$:\widetilde{J}^A(x):=\sum_{n=1}^{N}\sum_{\alpha,\beta}^{M}(T^A)_{\alpha\beta}:\psi_{n,\alpha}^\dagger(x)\psi_{n,\beta}(x):=\sum_{n=1}^{N}\sum_{\alpha,\beta}^{M}(T^A)_{\alpha\beta}\psi_{n,\alpha}^\dagger(x)\psi_{n,\beta}(x)=\widetilde{J}^A(x) \tag{C3}$$

where the normal order of fermions gives an expectation value with $\delta_{\alpha\beta}$ which was canceled by traceless $(T^A)_{\alpha\beta}$. The product of two current operators (with/without normal order) is

$$:\widetilde{J}^A(x)::\widetilde{J}^B(y):=\widetilde{J}^A(x)\widetilde{J}^B(y)=\sum_{i,j}\sum_{\alpha,\beta,\rho,\sigma}(T^A)_{\alpha\beta}(T^B)_{\rho\sigma}\psi_{i,\alpha}^\dagger(x)\psi_{i,\beta}(x)\psi_{j,\rho}^\dagger(y)\psi_{j,\sigma}(y). \tag{C4}$$

By Wick's theorem, the product for fermions is

$$\psi_{i,\alpha}^\dagger(x)\psi_{i,\beta}(x)\psi_{j,\rho}^\dagger(y)\psi_{j,\sigma}(y) \tag{C5}$$

$$=\psi_{i,\alpha}^\dagger(x):\psi_{i,\beta}(x)\psi_{j,\rho}^\dagger(y):\psi_{j,\sigma}(y)+\langle\psi_{i,\beta}(x)\psi_{j,\rho}^\dagger(y)\rangle\psi_{i,\alpha}^\dagger(x)\psi_{j,\sigma}(y) \tag{C6}$$

$$=:\psi_{i,\alpha}^\dagger(x)\psi_{i,\beta}(x)\psi_{j,\rho}^\dagger(y)\psi_{j,\sigma}(y):+\langle\psi_{i,\alpha}^\dagger(x)\psi_{j,\sigma}(y)\rangle:\psi_{i,\beta}(x)\psi_{j,\rho}^\dagger(y): \tag{C7}$$

$$+\langle\psi_{i,\beta}(x)\psi_{j,\rho}^\dagger(y)\rangle:\psi_{i,\alpha}^\dagger(x)\psi_{j,\sigma}(y):+\langle\psi_{i,\beta}(x)\psi_{j,\rho}^\dagger(y)\rangle\langle\psi_{i,\alpha}^\dagger(x)\psi_{j,\sigma}(y)\rangle \tag{C8}$$

$$=:\psi_{i,\alpha}^\dagger(x)\psi_{i,\beta}(x)\psi_{j,\rho}^\dagger(y)\psi_{j,\sigma}(y):+G(x-y)\delta_{ij}\delta_{\alpha\sigma}:\psi_{i,\beta}(x)\psi_{j,\rho}^\dagger(y): \tag{C9}$$

$$+G(x-y)\delta_{ij}\delta_{\beta\rho}:\psi_{i,\alpha}^\dagger(x)\psi_{j,\sigma}(y):+G^2(x-y)\delta_{ij}^2\delta_{\alpha\sigma}\delta_{\beta\rho} \tag{C10}$$

where the contraction $\langle\psi_{i,\alpha}^\dagger(x)\psi_{i,\sigma}(y)\rangle=\langle\psi_{i,\alpha}(x)\psi_{j,\sigma}^\dagger(y)\rangle=G(x-y)\delta_{ij}\delta_{\alpha\sigma}$ is evaluated in Eq. (C16) below. Thus, we can find the commutator

$$[\widetilde{J}^A(x),\widetilde{J}^B(y)]=\sum_i\sum_{\alpha,\sigma}G(x-y)(T^BT^A)_{\alpha\sigma}:\psi_{i,\sigma}(x)\psi_{i,\alpha}^\dagger(y):-G(y-x)(T^BT^A)_{\alpha\sigma}:\psi_{i,\alpha}^\dagger(y)\psi_{i,\sigma}(x): \tag{C11}$$

$$+ G(x-y)(T^A T^B)_{\alpha\sigma} : \psi^\dagger_{i,\alpha}(x)\psi_{i,\sigma}(y) : -G(y-x)(T^A T^B)_{\alpha\sigma} : \psi_{i,\sigma}(y)\psi^\dagger_{i,\alpha}(x) : \tag{C12}$$

$$+ [G^2(x-y) - G^2(y-x)]N\mathrm{Tr}(T^A T^B). \tag{C13}$$

Here, as we can check $: \psi_{i,\sigma}(x)\psi^\dagger_{i,\alpha}(y) := - : \psi^\dagger_{i,\alpha}(y)\psi_{i,\sigma}(x) :$ for $\alpha \neq \sigma$. When $\alpha = \sigma$, we simply have

$$: \psi_{i,\alpha}(x)\psi^\dagger_{i,\alpha}(y) := \psi_{i,\alpha}(x)\psi^\dagger_{i,\alpha}(y) - G(x-y) = - : \psi^\dagger_{i,\alpha}(y)\psi_{i,\alpha}(x) : +\delta(x-y) - G(y-x) - G(x-y). \tag{C14}$$

The zero-temperature fermion Green's function is evaluated as follows. We start with

$$\langle \psi_{i,\alpha}(x)\psi^\dagger_{j,\sigma}(y)\rangle = \frac{1}{l}\sum_{p,p'} e^{ipx-ip'y}\langle c_{p,i\alpha}c^\dagger_{p',j\sigma}\rangle = \frac{1}{l}\sum_{p,p'} e^{ipx-ip'y}\delta_{ij}\delta_{\alpha\sigma}\delta_{pp'}\theta(p') = \frac{\delta_{ij}\delta_{\alpha\sigma}}{l}\sum_p e^{ip(x-y)}\theta(p). \tag{C15}$$

By definition, we have

$$G(x-y) = \frac{1}{l}\sum_p e^{ip(x-y)}\theta(p) = \frac{1}{2\pi}\lim_{\delta\to 0^+}\int_0^\infty dp\, e^{ip(x-y+i\delta)} = \frac{1}{2\pi}\lim_{\delta\to 0^+}\frac{i}{x-y+i\delta}. \tag{C16}$$

Thus,

$$G(x-y) + G(y-x) = \frac{1}{2\pi}\lim_{\delta\to 0^+}\frac{i}{x-y+i\delta} + \frac{i}{y-x+i\delta} = \delta(x-y), \tag{C17}$$

$$G^2(x-y) - G^2(y-x) = \frac{1}{4\pi^2}\lim_{\delta\to 0^+} -\frac{1}{(x-y+i\delta)^2} + \frac{1}{(y-x+i\delta)^2} = \frac{i}{2\pi}\partial_x\big[G(x-y) + G(y-x)\big]$$

$$= \frac{i}{2\pi}\partial_x\delta(x-y). \tag{C18}$$

From the equation above, we have $: \psi_{i,\sigma}(x)\psi^\dagger_{i,\alpha}(y) := - : \psi^\dagger_{i,\alpha}(y)\psi_{i,\sigma}(x) :$ for all α, σ. This means the first two lines of Eq. (C11, C12) can be combined as a commutator of T^A and T^B, which can be replaced by $i\sum_C f^{ABC}T^C$. The last term is simply

$$[G(x-y)^2 - G(y-x)^2]N\mathrm{Tr}(T^A T^B) = \frac{iN}{\pi}\partial_x\delta(x-y)\delta^{AB}. \tag{C19}$$

Finally, we have

$$\big[\widetilde{J}^A(x), \widetilde{J}^B(y)\big] = i\sum_C f^{ABC}\widetilde{J}^C(x)\delta(x-y) + \frac{iN}{\pi}\partial_x\delta(x-y)\delta^{AB}. \tag{C20}$$

By a Fourier transformation,

$$\widetilde{J}^A_p = \int_{-l}^l dx\, e^{ip\pi x/l}\,\widetilde{J}^A(x), \tag{C21}$$

the above commutator will satisfy the Kac-Moody algebra,

$$[\widetilde{J}^A_p, \widetilde{J}^B_{p'}] = \int_{-l}^l\int_{-l}^l dx\, dy\, e^{ip\pi x/l+ip'\pi y/l}\big[\widetilde{J}^A(x), \widetilde{J}^B(y)\big] \tag{C22}$$

$$= \int_{-l}^l\int_{-l}^l dx\, dy\, e^{ip\pi x/l+ip'\pi y/l}\big[i\sum_C f^{ABC}\widetilde{J}^C(x)\delta(x-y) + \frac{iN}{\pi}\partial_x\delta(x-y)\delta^{AB}\big] \tag{C23}$$

$$= i\sum_C f^{ABC}\widetilde{J}^C_{p+p'} + 2N\, p\delta^{AB}\delta_{p,-p'}. \tag{C24}$$

This is Eq. (11) of the main text. The integral for the second term is

$$\frac{iN}{\pi}\delta^{AB}\int_{-l}^l\int_{-l}^l dx\, dy\, e^{ip\pi x/l+ip'\pi y/l}\,\partial_x\delta(x-y) \tag{C25}$$

$$= \frac{iN}{\pi}\delta^{AB}\int_{-l}^l\int_{-l}^l dx\, dy\, \Big\{\partial_x\big[e^{ip\pi x/l+ip'\pi y/l}\,\delta(x-y)\big] - \frac{ip\pi}{l}e^{ip\pi x/l+ip'\pi y/l}\,\delta(x-y)\Big\} \tag{C26}$$

$$= \frac{Nk}{l} \delta^{AB} \int_{-l}^{l} \int_{-l}^{l} \mathrm{d}x \, \mathrm{d}y \, e^{\mathrm{i}p\pi x/l + \mathrm{i}p'\pi y/l} \delta(x - y) \tag{C27}$$

$$= \frac{Np}{l} \delta^{AB} \left(2l\delta_{p,-p'}\right) = 2N \, p\delta^{AB}\delta_{p,-p'}. \tag{C28}$$

The $SO(M)_1$ Kac-Moody algebra is defined to be

$$[\widetilde{J}_p^A, \widetilde{J}_{p'}^B] = \mathrm{i} \sum_C f^{ABC} \widetilde{J}_{p+p'}^C + p\delta^{AB}\delta_{p,-p'}. \tag{C29}$$

Appendix D: Primary states and fusion rules

The primary states, Eq. (D6), are the most fundamental states in the Kac-Moody algebra. Excited states can be constructed from primary states by using raising operators [45, 63]. Here, we use a general method to derive the allowed primary states (representations) in $SO(M)$. The fusion rules (including the single and double fusion with the impurity) and the energies of the allowed representations are also given for the $SO(4)_2$ case.

1. The representation cut off of $SO(4)_2$

The Kac-Moody algebra for $SO(4)_2$ [see Eq. (C29)] is

$$[\widetilde{J}_p^A, \widetilde{J}_{p'}^B] = \mathrm{i} \sum_C f^{ABC} \widetilde{J}_{p+p'}^C + 2p\delta^{AB}\delta_{p,-p'} \tag{D1}$$

where $A, B \in \{12, 13, 14, 23, 24, 34\}$ and we can define $A, B = 1, 2, 3, 4, 5, 6$ for simplicity. This gives

$$f^{1BC} = \begin{pmatrix} 0 & 0 & 0 & 0 & 0 & 0 \\ 0 & 0 & 0 & 1 & 0 & 0 \\ 0 & 0 & 0 & 0 & 1 & 0 \\ 0 & -1 & 0 & 0 & 0 & 0 \\ 0 & 0 & -1 & 0 & 0 & 0 \\ 0 & 0 & 0 & 0 & 0 & 0 \end{pmatrix}_{BC} ; f^{2BC} = \begin{pmatrix} 0 & 0 & 0 & -1 & 0 & 0 \\ 0 & 0 & 0 & 0 & 0 & 0 \\ 0 & 0 & 0 & 0 & 0 & 1 \\ 1 & 0 & 0 & 0 & 0 & 0 \\ 0 & 0 & 0 & 0 & 0 & 0 \\ 0 & 0 & -1 & 0 & 0 & 0 \end{pmatrix}_{BC} ; f^{3BC} = \begin{pmatrix} 0 & 0 & 0 & 0 & -1 & 0 \\ 0 & 0 & 0 & 0 & 0 & -1 \\ 0 & 0 & 0 & 0 & 0 & 0 \\ 0 & 0 & 0 & 0 & 0 & 0 \\ 1 & 0 & 0 & 0 & 0 & 0 \\ 0 & 1 & 0 & 0 & 0 & 0 \end{pmatrix}_{BC} \tag{D2}$$

$$f^{4BC} = \begin{pmatrix} 0 & 1 & 0 & 0 & 0 & 0 \\ -1 & 0 & 0 & 0 & 0 & 0 \\ 0 & 0 & 0 & 0 & 0 & 0 \\ 0 & 0 & 0 & 0 & 0 & 0 \\ 0 & 0 & 0 & 0 & 0 & 1 \\ 0 & 0 & 0 & 0 & -1 & 0 \end{pmatrix}_{BC} ; f^{5BC} = \begin{pmatrix} 0 & 0 & 1 & 0 & 0 & 0 \\ 0 & 0 & 0 & 0 & 0 & 0 \\ -1 & 0 & 0 & 0 & 0 & 0 \\ 0 & 0 & 0 & 0 & 0 & -1 \\ 0 & 0 & 0 & 0 & 0 & 0 \\ 0 & 0 & 1 & 0 & 0 \end{pmatrix}_{BC} ; f^{6BC} = \begin{pmatrix} 0 & 0 & 0 & 0 & 0 & 0 \\ 0 & 0 & 1 & 0 & 0 & 0 \\ 0 & -1 & 0 & 0 & 0 & 0 \\ 0 & 0 & 0 & 0 & 1 & 0 \\ 0 & 0 & 0 & -1 & 0 & 0 \\ 0 & 0 & 0 & 0 & 0 & 0 \end{pmatrix}_{BC} . \tag{D3}$$

In the following, we write $\widetilde{J}$ as J for simplicity. The lowering operators are

$$F_p^{-1,1} = \frac{1}{2}[J_p^{13} + iJ_p^{14} - i(J_p^{23} + iJ_p^{24})]; \quad F_p^{-1,-1} = \frac{1}{2}[J_p^{13} - iJ_p^{14} - i(J_p^{23} - iJ_p^{24})]. \tag{D4}$$

The raising operators are

$$F_p^{1,1} = \frac{1}{2}[J_p^{13} + iJ_p^{14} + i(J_p^{23} + iJ_p^{24})]; \quad F_p^{1,-1} = \frac{1}{2}[J_p^{13} - iJ_p^{14} + i(J_p^{23} - iJ_p^{24})]. \tag{D5}$$

The highest-weight primary states $|\ell_1, \ell_2\rangle$ are defined to have the following properties:

$$\text{primary states: } J_p^A|\ell_1, \ell_2\rangle = 0, \text{ for } p > 0; \tag{D6}$$

$$\text{highest wight : } F_0^{1,1}|\ell_1, \ell_2\rangle = 0 \text{ and } F_0^{1,-1}|\ell_1, \ell_2\rangle = 0; \tag{D7}$$

$$\text{eigenstates of Cartan generators : } H_0^i|\ell_1, \ell_2\rangle = \ell_i|\ell_1, \ell_2\rangle. \tag{D8}$$

In order to derive the bound for the values of $\ell_{1,2}$, we consider two excited states $F_{-1}^{1,1}|\ell_1, \ell_2\rangle$ and $F_{-1}^{1,-1}|\ell_1, \ell_2\rangle$ by acting on all the two raising operators (positive roots) above. Their norms should be non-negative, which are

$$\langle \ell_1, \ell_2 | F_1^{-1,-1} F_{-1}^{1,1} | \ell_1, \ell_2\rangle = \langle \ell_1, \ell_2 | [F_1^{-1,-1}, F_{-1}^{1,1}] | \ell_1, \ell_2\rangle$$

$$=\langle\ell_1,\ell_2|(2-H_0^1-H_0^2)|\ell_1,\ell_2\rangle=2-\ell_1-\ell_2\geq 0 \tag{D9}$$

and

$$\langle\ell_1,\ell_2|F_1^{-1,1}F_{-1}^{1,-1}|\ell_1,\ell_2\rangle=\langle\ell_1,\ell_2|[F_1^{-1,1}F_{-1}^{1,-1}]|\ell_1,\ell_2\rangle$$
$$=\langle\ell_1,\ell_2|(2-H_0^1+H_0^2)|\ell_1,\ell_2\rangle=2-\ell_1+\ell_2\geq 0 \tag{D10}$$

where we used the following Kac-Moody algebra

$$[F_1^{-1,-1},F_{-1}^{1,1}]=\frac{1}{4}\big[J_1^{13}-\mathrm{i}J_1^{14}-\mathrm{i}(J_1^{23}-\mathrm{i}J_1^{24}),\ J_{-1}^{13}+\mathrm{i}J_{-1}^{14}+\mathrm{i}(J_{-1}^{23}+\mathrm{i}J_{-1}^{24})\big] \tag{D11}$$

$$=\frac{1}{4}\Big\{4\times 2+\mathrm{i}[J_1^{13},J_{-1}^{14}]+\mathrm{i}[J_1^{13},J_{-1}^{23}]-[J_1^{13},J_{-1}^{24}] \tag{D12}$$

$$-\mathrm{i}[J_1^{14},J_{-1}^{13}]+[J_1^{14},J_{-1}^{23}]+\mathrm{i}[J_1^{14},J_{-1}^{24}] \tag{D13}$$

$$-\mathrm{i}[J_1^{23},J_{-1}^{13}]+[J_1^{23},J_{-1}^{14}]+\mathrm{i}[J_1^{23},J_{-1}^{24}] \tag{D14}$$

$$-[J_1^{24},J_{-1}^{13}]-\mathrm{i}[J_1^{24},J_{-1}^{14}]-\mathrm{i}[J_1^{24},J_{-1}^{23}]\Big\} \tag{D15}$$

$$=2+\frac{1}{4}\Big\{2\mathrm{i}[J_1^{13},J_{-1}^{14}]+2\mathrm{i}[J_1^{13},J_{-1}^{23}]+2\mathrm{i}[J_1^{14},J_{-1}^{24}]+2\mathrm{i}[J_1^{23},J_{-1}^{24}]\Big\} \tag{D16}$$

$$=2-\frac{1}{2}J_0^{34}-\frac{1}{2}J_0^{12}-\frac{1}{2}J_0^{12}-\frac{1}{2}J_0^{34}=2-H_0^1-H_0^2 \tag{D17}$$

and

$$[F_1^{-1,1},F_{-1}^{1,-1}]=\frac{1}{4}\big[J_1^{13}+\mathrm{i}J_1^{14}-\mathrm{i}(J_1^{23}+\mathrm{i}J_1^{24}),\ J_{-1}^{13}-\mathrm{i}J_{-1}^{14}+\mathrm{i}(J_{-1}^{23}-\mathrm{i}J_{-1}^{24})\big] \tag{D18}$$

$$=\frac{1}{4}\Big\{4\times 2-\mathrm{i}[J_1^{13},J_{-1}^{14}]+\mathrm{i}[J_1^{13},J_{-1}^{23}]-[J_1^{13},J_{-1}^{24}] \tag{D19}$$

$$+\mathrm{i}[J_1^{14},J_{-1}^{13}]-[J_1^{14},J_{-1}^{23}]+\mathrm{i}[J_1^{14},J_{-1}^{24}] \tag{D20}$$

$$-\mathrm{i}[J_1^{23},J_{-1}^{13}]-[J_1^{23},J_{-1}^{14}]-\mathrm{i}[J_1^{23},J_{-1}^{24}] \tag{D21}$$

$$+[J_1^{24},J_{-1}^{13}]-\mathrm{i}[J_1^{24},J_{-1}^{14}]+\mathrm{i}[J_1^{24},J_{-1}^{23}]\Big\} \tag{D22}$$

$$=2+\frac{1}{4}\Big\{-2\mathrm{i}[J_1^{13},J_{-1}^{14}]+2\mathrm{i}[J_1^{13},J_{-1}^{23}]+2\mathrm{i}[J_1^{14},J_{-1}^{24}]-2\mathrm{i}[J_1^{23},J_{-1}^{24}]\Big\} \tag{D23}$$

$$=2+\frac{1}{2}J_0^{34}-\frac{1}{2}J_0^{12}-\frac{1}{2}J_0^{12}+\frac{1}{2}J_0^{34}=2-H_0^1+H_0^2. \tag{D24}$$

The above results from the Lie algebra satisfy $[F^{\vec{\alpha}},F^{-\vec{\alpha}}]=\vec{\alpha}\cdot\vec{H}$ (see Howard Georgi's Lie algebra textbook [50] and the Chapter 14 of Ref. [64]), which can be used for further generalization with $\mathrm{SO}(M)_k$. In terms of the highest weights of the fundamental representation $\mu_1=(1/2,1/2)$ and $\mu_2=(1/2,-1/2)$, we get

$$(\ell_1,\ell_2)=(\ell_1+\ell_2)\mu_1+(\ell_1-\ell_2)\mu_2. \tag{D25}$$

As we know, the highest weight of any representation can be written as $a_1\mu_1+a_2\mu_2$, i.e., the sum of the fundamental ones with $a_i\in\mathbb{Z}_{\geq 0}$. Thus, the two requirements Eq. (D9) and Eq. (D10) are equivalent to $a_{1,2}\leq 2$, which can be considered as the requirements of two $\mathrm{SU}(2)_2$.

2. The representation cut off for $\mathrm{SO}(2m)_k$

For $\mathrm{SO}(2m)_k$, the two fundamental spinor representations are μ_{m-1} and μ_m. The $m(m-1)$ positive roots are $e_i\pm e_j\ i<j=1,...,m$ where $e_i=(0,..,1,..,0)$ which has 1 at the ith position and 0 elsewhere. The simple roots are e_i-e_{i+1}, $i=1,m-1$ and $e_{m-1}+e_m$. By considering the $m(m-1)$ lowering operators acting on the state $|\vec{\ell}\rangle$ for all the positive roots and requiring the new states to have non-negative norm [same as we did in Eq. (D9) and Eq. (D10)], we get constrains for ℓs:

$$\ell_i\pm\ell_j\leq k,\ i<j=1,...,m. \tag{D26}$$

Thus, in terms of $\vec{\ell}=\sum_{i=1}^m a_i\mu_i$ with the fundamental weights

$$\mu_1=(1,0,0,...,0,0,0), \tag{D27}$$

$$\mu_2 = (1, 1, 0, ..., 0, 0, 0), \tag{D28}$$

$$\mu_3 = (1, 1, 1, ..., 0, 0, 0), \tag{D29}$$

$$\vdots \tag{D30}$$

$$\mu_{m-2} = (1, 1, 1, ..., 1, 0, 0), \tag{D31}$$

$$\mu_{m-1} = \frac{1}{2}(1, 1, 1, ..., 1, 1, -1), \tag{D32}$$

$$\mu_m = \frac{1}{2}(1, 1, 1, ..., 1, 1, 1), \tag{D33}$$

we get

$$\ell_i = \sum_{n=i}^{m-2} a_i + \frac{1}{2}a_{m-1} + \frac{1}{2}a_m, \ i = 1, m-2; \tag{D34}$$

$$\ell_{m-1} = \frac{1}{2}a_{m-1} + \frac{1}{2}a_m; \ \ell_m = -\frac{1}{2}a_{m-1} + \frac{1}{2}a_m \tag{D35}$$

and inversely

$$a_i = \ell_i - \ell_{i+1}, \ i = 1, ..., m-1; \ a_m = \ell_{m-1} + \ell_m. \tag{D36}$$

Thus, the simple roots give $a_{i=1,...,m} \leq k$.

For the case of $SO(6)_k$, we have 15 generators, which are 3 Cartan generators, 6 positive roots and 6 negative roots. The above representation cut off is generally given by considering $F_{-1}^{\alpha_1, \alpha_2, \alpha_3}|\ell_1, \ell_2, \ell_3\rangle$ when $\vec{\alpha} = (\alpha_1, \alpha_2, \alpha_3)$ are the positive roots. Here, we give all the positive roots:

$$\vec{\alpha} = (1, -1, 0), \ \vec{\beta} = (0, 1, -1), \ \vec{\rho} = (0, 1, 1), \tag{D37}$$

$$\vec{\alpha} + \vec{\beta} = (1, 0, -1), \ \vec{\alpha} + \vec{\rho} = (1, 0, 1), \ \vec{\alpha} + \vec{\beta} + \vec{\rho} = (1, 1, 0) \tag{D38}$$

where the upper line gives 3 simple roots. By calculating the norm of $F_{-1}^{\alpha_1, \alpha_2, \alpha_3}|\ell_1, \ell_2, \ell_3\rangle$ and the commutator $[F^{\vec{\alpha}}, F^{-\vec{\alpha}}] = \vec{\alpha} \cdot \vec{H}$, we get the requirements correspondingly for each postive root:

$$\ell_1 - \ell_2 \leq k, \ \ell_2 - \ell_3 \leq k, \ \ell_2 + \ell_3 \leq k \tag{D39}$$

$$\ell_1 - \ell_3 \leq k, \ \ell_1 + \ell_3 \leq k, \ \ell_1 + \ell_2 \leq k. \tag{D40}$$

In terms of Dynkin labels $a_{i=1,2,3}$, we have $(\ell_1, \ell_2, \ell_3) = a_1\xi_1 + a_2\xi_2 + a_3\xi_3$ with

$$\xi_1 = (1, 0, 0), \ \xi_2 = (\frac{1}{2}, \frac{1}{2}, \frac{1}{2}), \ \xi_3 = (\frac{1}{2}, \frac{1}{2}, -\frac{1}{2}); \tag{D41}$$

$$a_1 = \ell_1 - \ell_2, \ a_2 = \ell_2 - \ell_3, \ a_3 = \ell_2 + \ell_3. \tag{D42}$$

Thus, we get requirements for the Dynkin labels $a_{i=1,2,3}$:

$$a_{1,2,3} \leq k; \ a_1 + a_2 \leq k; \ a_1 + a_3 \leq k; \ a_1 + a_2 + a_3 \leq k. \tag{D43}$$

3. The representation cut off for $SO(2m+1)_k$

For $SO(2m+1)_k$, the only fundamental spinor representation is ξ_m. The m^2 positive roots are $e_i \pm e_j$ and e_j with $i < j = 1, ..., m$. The simple roots are $e_i - e_{i+1}$, $i = 1, m-1$ and e_m. This gives the requirements for ℓs:

$$\ell_i \pm \ell_j \leq k \text{ and } \ell_j \leq k, \ i < j = 1, ..., m. \tag{D44}$$

Thus, in terms of $\vec{\ell} = \sum_{i=1}^{m} a_i\xi_i$ with the fundamental weights

$$\mu_1 = (1, 0, 0, ..., 0, 0, 0), \tag{D45}$$

$$\mu_2 = (1, 1, 0, ..., 0, 0, 0), \tag{D46}$$

$$\mu_3 = (1, 1, 1, ..., 0, 0, 0), \tag{D47}$$

$$\vdots \tag{D48}$$

$$\mu_{m-2} = (1, 1, 1, ..., 1, 0, 0), \tag{D49}$$

$$\mu_{m-1} = (1, 1, 1, ..., 1, 1, 0), \tag{D50}$$

$$\mu_m = \frac{1}{2}(1, 1, 1, ..., 1, 1, 1) \tag{D51}$$

we get

$$\ell_i = \sum_{n=i}^{m-1} a_n + \frac{1}{2}a_m, \ i = 1, m-1; \ \ell_m = \frac{1}{2}a_m \tag{D52}$$

and inversely

$$a_i = \ell_i - \ell_{i+1}, \ i = 1, ..., m-1; \ a_m = 2\ell_m. \tag{D53}$$

Thus, the simple roots give $a_{i=1,...,m-1} \leq k$ and $a_m \leq 2k$.

4. The fusion rule of SO$(4)_2$

According to the above cut off (see Sec. D 1), the allowed representations for SO$(4)_2$ are

$$\text{spinor}: \mu_1, \mu_2, 2\mu_1 + \mu_2, \mu_1 + 2\mu_2; \tag{D54}$$

$$\text{vector}: 0, \mu_1 + \mu_2, 2\mu_1, 2\mu_2, 2\mu_1 + 2\mu_2. \tag{D55}$$

Their fusion rules are

$$\mu_1 \otimes \mu_1 = 2\mu_1 \oplus 0; \ \mu_1 \otimes \mu_2 = \mu_1 + \mu_2; \tag{D56}$$

$$\mu_1 \otimes (\mu_1 + \mu_2) = (2\mu_1 + \mu_2) \oplus \mu_2; \ \mu_1 \otimes 2\mu_1 = \cancel{3\mu_1} \oplus \mu_1; \ \mu_1 \otimes 2\mu_2 = (\mu_1 + 2\mu_2); \tag{D57}$$

$$\mu_1 \otimes (2\mu_1 + \mu_2) = \cancel{(3\mu_1 + \mu_2)} \oplus (\mu_1 + \mu_2); \ \mu_1 \otimes (\mu_1 + 2\mu_2) = (2\mu_1 + 2\mu_2) \oplus (2\mu_2); \tag{D58}$$

$$\mu_1 \otimes (2\mu_1 + 2\mu_2) = \cancel{(3\mu_1 + 2\mu_2)} \oplus (\mu_1 + 2\mu_2); \tag{D59}$$

$$\mu_2 \otimes \mu_2 = 2\mu_2 \oplus 0; \tag{D60}$$

$$\mu_2 \otimes (\mu_1 + \mu_2) = (\mu_1 + 2\mu_2) \oplus \mu_1; \ \mu_2 \otimes 2\mu_1 = 2\mu_1 + \mu_2; \ \mu_2 \otimes 2\mu_2 = \cancel{3\mu_2} \oplus \mu_2; \tag{D61}$$

$$\mu_2 \otimes (2\mu_1 + \mu_2) = (2\mu_1 + 2\mu_2) \oplus 2\mu_1; \ \mu_2 \otimes (\mu_1 + 2\mu_2) = \cancel{(\mu_1 + 3\mu_2)} \oplus (\mu_1 + \mu_2); \tag{D62}$$

$$\mu_2 \otimes (2\mu_1 + 2\mu_2) = \cancel{(2\mu_1 + 3\mu_2)} \oplus (2\mu_1 + \mu_2); \tag{D63}$$

$$(\mu_1 + \mu_2) \otimes (\mu_1 + \mu_2) = (2\mu_1 + 2\mu_2) \oplus 2\mu_1 \oplus 2\mu_2 \oplus 0; \tag{D64}$$

$$(\mu_1 + \mu_2) \otimes 2\mu_1 = \cancel{3\mu_1} \oplus \mu_1 \oplus (2\mu_1 + \mu_2); \tag{D65}$$

$$(\mu_1 + \mu_2) \otimes 2\mu_2 = (\mu_1 + 2\mu_2) \oplus \cancel{3\mu_2} \oplus \mu_2; \tag{D66}$$

$$(\mu_1 + \mu_2) \otimes (2\mu_1 + \mu_2) = \cancel{(3\mu_1 + 2\mu_2)} \oplus \cancel{3\mu_1} \oplus (\mu_1 + 2\mu_2) \oplus \mu_1; \tag{D67}$$

$$(\mu_1 + \mu_2) \otimes (\mu_1 + 2\mu_2) = \cancel{(2\mu_1 + 3\mu_2)} \oplus \cancel{3\mu_2} \oplus (2\mu_1 + \mu_2) \oplus \mu_2; \tag{D68}$$

$$(\mu_1 + \mu_2) \otimes (2\mu_1 + 2\mu_2) = \cancel{(3\mu_1 + 3\mu_2)} \oplus \cancel{(3\mu_1 + \mu_2)} \oplus \cancel{(\mu_1 + 3\mu_2)} \oplus (\mu_1 + \mu_2); \tag{D69}$$

$$2\mu_1 \otimes 2\mu_1 = \cancel{4\mu_1} \oplus 0; \ 2\mu_1 \otimes 2\mu_2 = (2\mu_1 + 2\mu_2); \tag{D70}$$

$$2\mu_1 \otimes (2\mu_1 + \mu_2) = \cancel{(4\mu_1 + \mu_2)} \oplus \mu_2; \tag{D71}$$

$$2\mu_1 \otimes (\mu_1 + 2\mu_2) = \cancel{(3\mu_1 + 2\mu_2)} \oplus (\mu_1 + 2\mu_2); \tag{D72}$$

$$2\mu_1 \otimes (2\mu_1 + 2\mu_2) = \cancel{(4\mu_1 + 2\mu_2)} \oplus 2\mu_2; \tag{D73}$$

$$2\mu_2 \otimes 2\mu_2 = \cancel{4\mu_2} \oplus 0; \tag{D74}$$

$$2\mu_2 \otimes (2\mu_1 + \mu_2) = \cancel{(2\mu_1 + 3\mu_2)} \oplus (2\mu_1 + \mu_2); \tag{D75}$$

Reps	0	μ_1	μ_2	$\mu_1 + \mu_2$	$2\mu_1$	$2\mu_2$	$2\mu_1 + \mu_2$	$\mu_1 + 2\mu_2$	$2\mu_1 + 2\mu_2$
Q-dim	1	$\sqrt{2}$	$\sqrt{2}$	2	1	1	$\sqrt{2}$	$\sqrt{2}$	1

TABLE V. The quantum dimensions for all the allowed representations in $\mathrm{SO}(4)_2$.

$$2\mu_2 \otimes (\mu_1 + 2\mu_2) = (\mu_1 + 4\mu_2) \oplus \mu_1; \tag{D76}$$

$$2\mu_2 \otimes (2\mu_1 + 2\mu_2) = (2\mu_1 + 4\mu_2) \oplus 2\mu_1; \tag{D77}$$

$$(2\mu_1 + \mu_2) \otimes (2\mu_1 + \mu_2) = (4\mu_1 + 2\mu_2) \oplus 4\mu_1 \oplus 2\mu_2 \oplus 0; \tag{D78}$$

$$(2\mu_1 + \mu_2) \otimes (\mu_1 + 2\mu_2) = (3\mu_1 + 3\mu_2) \oplus (3\mu_1 + \mu_2) \oplus (\mu_1 + 3\mu_2) \oplus (\mu_1 + \mu_2); \tag{D79}$$

$$(2\mu_1 + \mu_2) \otimes (2\mu_1 + 2\mu_2) = (4\mu_1 + 3\mu_2) \oplus (4\mu_1 + \mu_2) \oplus 3\mu_2 \oplus \mu_2; \tag{D80}$$

$$(\mu_1 + 2\mu_2) \otimes (\mu_1 + 2\mu_2) = (2\mu_1 + 4\mu_2) \oplus 4\mu_2 \oplus 2\mu_1 \oplus 0; \tag{D81}$$

$$(\mu_1 + 2\mu_2) \otimes (2\mu_1 + 2\mu_2) = (3\mu_1 + 4\mu_2) \oplus (\mu_1 + 4\mu_2) \oplus 3\mu_1 \oplus \mu_1; \tag{D82}$$

$$(2\mu_1 + 2\mu_2) \otimes (2\mu_1 + 2\mu_2) = (4\mu_1 + 4\mu_2) \oplus 4\mu_1 \oplus 4\mu_2 \oplus 0. \tag{D83}$$

The above crossed terms will not be allowed in the fusion rules, but will appear in the representation decompositions. The (matrix) representation dimensions are always integers when the above crossed terms are kept. However, the effective "dimensions", i.e. the quantum dimensions are non-integers in the above fusion rules where the crossed terms are absent. In order to obtain the quantum dimensions, we first assume that the quantum dimensions of the above representations are $d_{Q,i=1,\ldots,9}$ and solve them from algebraic equations. The equations are given by the above fusion rules, i.e., the product of quantum dimensions for the left-side representations equals the sum of quantum dimensions for the right-side representations. The solutions for the quantum dimensions $d_{Q,i=1,\ldots,9}$ are listed in Table V. The general result for the above representations $a_1\mu_1 + a_2\mu_2$ is

$$d_Q(a_1, a_2) = \begin{cases} 1 & (\widetilde{a_1}, \widetilde{a_2}) = (0,0) \\ \sqrt{2} & (\widetilde{a_1}, \widetilde{a_2}) = (0,1) \text{ or } (1,0) \\ 2 & (\widetilde{a_1}, \widetilde{a_2}) = (1,1) \end{cases}, \quad \widetilde{a_i} = \min(a_i, 2 - a_i). \tag{D84}$$

More general result can be found for $\mathrm{SO}(4)_k$

$$d_Q^{\mathrm{SO}(4)_k}(a_1, a_2) = d^{\mathrm{SU}(2)_k}(a_1) \times d^{\mathrm{SU}(2)_k}(a_2); \quad d^{\mathrm{SU}(2)_k}(a_i) = \frac{\sin[\pi(a_i + 1)/(k + 2)]}{\sin[\pi/(k + 2)]} \tag{D85}$$

which explains how the $\mathrm{SO}(4)_k$ anyons are related to two copies of $\mathrm{SU}(2)_k$ anyons due to the fact $\mathrm{SO}(4) \sim \mathrm{SU}(2) \times \mathrm{SU}(2)$. This may be possible to generalize for any classical Lie group at any level because they all have $\mathrm{SU}(2)$ subalgebras.

5. Energies of $\mathrm{SO}(4)_2$

Following Ludwig's lecture notes [45, 63] and Ref. [34], we get the Hamiltonian

$$H_0 = H_{\mathrm{SO}(4)_2} + H_{\mathrm{SO}(2)_4} \tag{D86}$$

$$= \frac{\pi v_F}{l} \sum_{p=-\infty}^{+\infty} \left\{ \frac{1}{2 + h^\vee[\mathrm{SO}(4)]} : J_{-p}^a J_p^a : + \frac{1}{4 + h^\vee[\mathrm{SO}(2)]} : J_{-p}^A J_p^A : \right\} \tag{D87}$$

$$= \frac{\pi v_F}{l} \sum_{p=-\infty}^{+\infty} \left\{ \frac{1}{2 + 2} : J_{-p}^a J_p^a : + \frac{1}{4 + 0} : J_{-p}^A J_p^A : \right\}. \tag{D88}$$

The $\mathrm{SO}(2)$ has only one generator $J_0^{A=1}$ that is a Cartan generator, which is like $\mathrm{U}(1)$. Thus, we define the highest wight primary state as $|Q\rangle$ and get : $J_{-p}^A J_p^A : |Q\rangle = Q^2 |Q\rangle$ where Q is the eigenvalue of $J_0^{A=1}$. If the representation of $\mathrm{SO}(4)$ are given by $a_1\mu_1 + a_2\mu_2$, we get

$$E - E^{(0)} = \frac{\pi v_F}{l} \left\{ \frac{1}{4}\frac{1}{2}\left[a_1 + \frac{a_1^2}{2} + a_2 + \frac{a_2^2}{2}\right] + \frac{1}{4}\frac{1}{2}Q^2 \right\} + \ldots. \tag{D89}$$

a_1	a_2	$Q \bmod 4$	$l\big[E - E^{(0)}\big]/\pi v_F$	n
0	0	0	0	1
1	1	1	1/2	1
2	0	2	1	1
0	2	2	1	1
2	2	0	1	1
1	1	3	3/2	1

TABLE VI. Table for the primary states and their energies/scaling dimensions at the free case for $SO(4)_2$.

If we take $a_1 = 2j$ and $a_2 = 2j_f$, we get

$$E - E^{(0)} = \frac{\pi v_F}{l}\left\{\frac{1}{4}\left(j + j^2 + j_f + j_f^2\right) + \frac{Q^2}{8}\right\} + \dots \tag{D90}$$

which is identical to the $SU(2)_2$ result.

6. Single fusion with the impurity for $SO(4)_2$

The representation for the impurity is $\mu_1 \oplus \mu_2$. We consider the single fusion of the impurity μ_1 (μ_2 is similar) with the above primary states. The results are listed in Table VII.

a_1	a_2	$Q \bmod 4$	$l\big[E - E^{(0)}\big]/\pi v_F$	n
1	0	0	3/16	1
0	1	1	5/16	1
2	1	1	13/16	1
1	0	2	11/16	1
1	2	2	19/16	1
1	2	0	11/16	1
0	1	3	21/16	1
2	1	3	29/16	1

TABLE VII. Table for the primary boundary operators and their energies/scaling dimensions at the Kondo fixed point for $SO(4)_2$ obtained by single fusion with the impurity μ_1. The single fusion results with impurity μ_2 can be found by interchanging $a_1 \leftrightarrow a_2$.

7. Double fusion with the impurity for $SO(4)_2$

The representation for the impurity is $\mu_1 \oplus \mu_2$. We consider the double fusion of the impurity with the above primary states shown in Table VI and allow the cross terms like $\mu_{1,2}$ from the first fusion with the impurity $\mu_1 \oplus \mu_2$ and $\mu_{2,1}$ from the second fusion with the impurity $\mu_1 \oplus \mu_2$. This is equivalent to not fixing the charge parity of the impurity. The double fusion results are in the following:

$$[\mu_1 \oplus \mu_2] \otimes [\mu_1 \oplus \mu_2] \otimes 0 = 2\mu_1 \oplus 0 \oplus 2\mu_2 \oplus 0 \oplus (\mu_1 + \mu_2) \oplus (\mu_1 + \mu_2); \tag{D91}$$

$$[\mu_1 \oplus \mu_2] \otimes [\mu_1 \oplus \mu_2] \otimes (\mu_1 + \mu_2) = [2\mu_1 \oplus 0 \oplus 2\mu_2 \oplus 0 \oplus (\mu_1 + \mu_2) \oplus (\mu_1 + \mu_2)] \otimes (\mu_1 + \mu_2) \tag{D92}$$
$$= \mu_1 \oplus (2\mu_1 + \mu_2) \oplus (\mu_1 + \mu_2) \oplus (\mu_1 + 2\mu_2) \oplus \mu_2 \oplus (\mu_1 + \mu_2) \oplus (2\mu_1 + 2\mu_2) \oplus 2\mu_1 \oplus 2\mu_2 \oplus 0 \tag{D93}$$
$$\oplus (2\mu_1 + 2\mu_2) \oplus 2\mu_1 \oplus 2\mu_2 \oplus 0; \tag{D94}$$

$$[\mu_1 \oplus \mu_2] \otimes [\mu_1 \oplus \mu_2] \otimes 2\mu_1 = [2\mu_1 \oplus 0 \oplus 2\mu_2 \oplus 0 \oplus (\mu_1 + \mu_2) \oplus (\mu_1 + \mu_2)] \otimes 2\mu_1 \tag{D95}$$
$$= 0 \oplus 2\mu_1 \oplus (2\mu_1 + 2\mu_2) \oplus 2\mu_1 \oplus \mu_1 \oplus (2\mu_1 + \mu_2) \oplus \mu_1 \oplus (2\mu_1 + \mu_2); \tag{D96}$$

$$[\mu_1 \oplus \mu_2] \otimes [\mu_1 \oplus \mu_2] \otimes 2\mu_2 = [2\mu_1 \oplus 0 \oplus 2\mu_2 \oplus 0 \oplus (\mu_1 + \mu_2) \oplus (\mu_1 + \mu_2)] \otimes 2\mu_2 \tag{D97}$$

a_1	a_2	$Q \bmod 4$	$l\left[E - E^{(0)}\right]/\pi v_F$	n
0	0	0	0	2
1	1	0	3/8	2
2	0	0	1/2	1
0	2	0	1/2	1
0	0	1	1/8	2
1	0	1	5/16	1
0	1	1	5/16	1
1	1	1	1/2	2
2	0	1	5/8	2
0	2	1	5/8	2
2	1	1	13/16	1
1	2	1	13/16	1
2	2	1	9/8	2
0	0	2	1/2	1
1	0	2	11/16	2
2	0	2	1	2
2	1	2	19/16	2
2	2	2	3/2	1
0	0	2	1/2	1
0	1	2	11/16	2
0	2	2	1	2
1	2	2	19/16	2
2	2	2	3/2	1
1	1	0	3/8	2
2	0	0	1/2	1
0	2	0	1/2	1
2	2	0	1	2
0	0	3	$1 + 1/8$	2
1	0	3	$1 + 5/16$	1
0	1	3	$1 + 5/16$	1
1	1	3	$1 + 1/2$	2
2	0	3	$1 + 5/8$	2
0	2	3	$1 + 5/8$	2
2	1	3	$1 + 13/16$	1
1	2	3	$1 + 13/16$	1
2	2	3	$1 + 9/8$	2

TABLE VIII. Table for the primary boundary operators and their energies/scaling dimensions at the Kondo fixed point for SO(4)$_2$ obtained by double fusion with the impurity. The red representations will not appear in the double fusion results if we fix the parity.

$$=(2\mu_1 + 2\mu_2) \oplus 2\mu_2 \oplus 0 \oplus 2\mu_2 \oplus (\mu_1 + 2\mu_2) \oplus \mu_2 \oplus (\mu_1 + 2\mu_2) \oplus \mu_2; \tag{D98}$$

$$[\mu_1 \oplus \mu_2] \otimes [\mu_1 \oplus \mu_2] \otimes (2\mu_1 + 2\mu_2) = [2\mu_1 \oplus 0 \oplus 2\mu_2 \oplus 0 \oplus (\mu_1 + \mu_2) \oplus (\mu_1 + \mu_2)] \otimes (2\mu_1 + 2\mu_2) \tag{D99}$$
$$=2\mu_2 \oplus (2\mu_1 + 2\mu_2) \oplus 2\mu_1 \oplus (2\mu_1 + 2\mu_2) \oplus (\mu_1 + \mu_2) \oplus (\mu_1 + \mu_2). \tag{D100}$$

Thus, we get Table VIII. The red representations will not appear in the double fusion results if we fix the parity. If we do not fix the parity, the primary operators $\phi_\alpha^{(a_1=1,a_2=1,Q=0)}$ have the smallest scaling dimension 3/8 in the table. However, we can not construct a set of operators that from this representation $a_1 = a_2 = 1$ using the generators $\vec{J}^{(0,2)}$. Thus, the leading irrelevant operator will be $\vec{J}_{-1}^{(0,2)} \cdot \vec{\phi}^{(0,2)} + \vec{J}_{-1}^{(2,0)} \cdot \vec{\phi}^{(2,0)}$ where $\vec{\phi}^{(2,0)}$ are the three $2\mu_1$-primary operators and $\vec{J}^{(2,0)}$ are the $2\mu_1$-operators [three generators of all the six generators for SO(4) and the other three operators are $\vec{J}^{(0,2)}$]. This leading irrelevant operator has scaling dimension $1 + 1/2 = 3/2$ becayse the primary operators $\vec{\phi}^{(0,2)}$ and $\vec{\phi}^{(2,0)}$ both have scaling dimension 1/2. If we fix the parity, we still use these two primary operators $\vec{\phi}^{(0,2)}$ and $\vec{\phi}^{(2,0)}$ to form the same leading irrelevant operator.

Appendix E: The representation of the density $J^{(d)}$

In Sec. IV A, we defined $J_\chi^{(d)}(x) = \sum_j \vec{\psi}_{\chi;j}^\dagger(x) D_1 \vec{\psi}_{\chi;j}(x)$ where $D_1 = \mathrm{diag}(1, -1, 0, \ldots, 0)$. The sum over channel index j means that $J^{(d)}$ is a singlet in the channel sector. In the flavor [SO(M)] sector, a general form for a density operator is $\sum_{ab} c_a^\dagger B_{ab}^\alpha c_b$ where $a, b = 1, \ldots, M$. One finds that there are three sets of them: the first one is given by $B^1 = \mathbb{I}_{M \times M}$, a symmetric traceful matrix; the second set of densities are the $[M(M-1)/2]$ antisymmetric traceless matrices; the last set of densities are the $[(M-1) + M(M-1)/2]$ symmetric traceless matrices. The matrix D_1 is one of these $M - 1 + M(M-1)/2$ symmetric traceless $M \times M$ matrices. The representation of these three sets of densities can be determined by decomposition of two 1-particle representations (the 1-particle representation has dimension M), which are two $2\mu_1$s (spin-1s) for SO(3), two $\mu_1 + \mu_2$s for SO(4) [see Eq. (B3)] and two μ_1s for SO($M \geq 5$). These decompositions are listed in the following equation.

$$\begin{cases} 2\mu_1 \otimes 2\mu_1 = 4\mu_1 \oplus 2\mu_1 \oplus \mathbf{0}, & \text{for SO(3)} \\ (\mu_1 + \mu_2) \otimes (\mu_1 + \mu_2) = (2\mu_1 + 2\mu_2) \oplus 2\mu_1 \oplus 2\mu_2 \oplus \mathbf{0}, & \text{for SO(4)} \\ \mu_1 \otimes \mu_1 = 2\mu_1 \oplus 2\mu_2 \oplus \mathbf{0}, & \text{for SO(5)} \\ \mu_1 \otimes \mu_1 = 2\mu_1 \oplus (\mu_2 + \mu_3) \oplus \mathbf{0}, & \text{for SO(6)} \\ \mu_1 \otimes \mu_1 = 2\mu_1 \oplus \mu_2 \oplus \mathbf{0}, & \text{for SO}(M \geq 7). \end{cases} \tag{E1}$$

The $\mathbf{0}$ is the identity B^1. The first representations on the right side (also the representation of $J^{(d)}$) are for the $M - 1 + M(M-1)/2$ real traceless $M \times M$ matrices; The rest of them are for the $[M(M-1)/2]$ antisymmetric traceless (the adjoint) $M \times M$ matrices.